Handbook for Communicating Travel Time Reliability Through Graphics and Tables

DETAILS

0 pages | 8.5 x 11 | PAPERBACK
ISBN 978-0-309-43359-4 | DOI 10.17226/22400

AUTHORS

Institute of Transportation Research and Education

SHRP 2 Reliability Project L02

Handbook for Communicating Travel Time Reliability Through Graphics and Tables

George F. List, Billy Williams, and Nagui Rouphail
Institute for Transportation Research and Education
North Carolina State University

in association with

Rob Hranac, Tiffany Barkley, Eric Mai, and Armand Ciccarelli
Iteris/Berkeley Transportation Systems, Inc.

Lee Rodegerdts, Katie Pincus, and Brandon Nevers
Kittelson & Associates, Inc.

Alan F. Karr
National Institute of Statistical Sciences

Xuesong Zhou
University of Utah

Jeffrey Wojtowicz
Rensselaer Polytechnic Institute

Joseph Schofer
Northwestern University

Asad Khattak
Planitek

TRANSPORTATION RESEARCH BOARD
Washington, D.C.
2014
www.TRB.org

ACKNOWLEDGMENT
This work was sponsored by the Federal Highway Administration in cooperation with the American Association of State Highway and Transportation Officials. It was conducted in the second Strategic Highway Research Program, which is administered by the Transportation Research Board of the National Academies.

THE NATIONAL ACADEMIES

Advisers to the Nation on Science, Engineering, and Medicine

The **National Academy of Sciences** is a private, nonprofit, self-perpetuating society of distinguished scholars engaged in scientific and engineering research, dedicated to the furtherance of science and technology and to their use for the general welfare. On the authority of the charter granted to it by Congress in 1863, the Academy has a mandate that requires it to advise the federal government on scientific and technical matters. Dr. Ralph J. Cicerone is president of the National Academy of Sciences.

The **National Academy of Engineering** was established in 1964, under the charter of the National Academy of Sciences, as a parallel organization of outstanding engineers. It is autonomous in its administration and in the selection of its members, sharing with the National Academy of Sciences the responsibility for advising the federal government. The National Academy of Engineering also sponsors engineering programs aimed at meeting national needs, encourages education and research, and recognizes the superior achievements of engineers. Dr. C. D. (Dan) Mote, Jr., is president of the National Academy of Engineering.

The **Institute of Medicine** was established in 1970 by the National Academy of Sciences to secure the services of eminent members of appropriate professions in the examination of policy matters pertaining to the health of the public. The Institute acts under the responsibility given to the National Academy of Sciences by its congressional charter to be an adviser to the federal government and, upon its own initiative, to identify issues of medical care, research, and education. Dr. Victor J. Dzau is president of the Institute of Medicine.

The **National Research Council** was organized by the National Academy of Sciences in 1916 to associate the broad community of science and technology with the Academy's purposes of furthering knowledge and advising the federal government. Functioning in accordance with general policies determined by the Academy, the Council has become the principal operating agency of both the National Academy of Sciences and the National Academy of Engineering in providing services to the government, the public, and the scientific and engineering communities. The Council is administered jointly by both Academies and the Institute of Medicine. Dr. Ralph J. Cicerone and Dr. C.D. (Dan) Mote, Jr., are chair and vice chair, respectively, of the National Research Council.

The **Transportation Research Board** is one of six major divisions of the National Research Council. The mission of the Transportation Research Board is to provide leadership in transportation innovation and progress through research and information exchange, conducted within a setting that is objective, interdisciplinary, and multimodal. The Board's varied activities annually engage about 7,000 engineers, scientists, and other transportation researchers and practitioners from the public and private sectors and academia, all of whom contribute their expertise in the public interest. The program is supported by state transportation departments, federal agencies including the component administrations of the U.S. Department of Transportation, and other organizations and individuals interested in the development of transportation. **www.TRB.org**

www.national-academies.org

Contents

Acronyms

ATA	actual time of arrival
AVI	automated vehicle identification
AVL	automated vehicle location
CDF	cumulative density, or distribution, function
D2D	day-to-day (variations in travel times)
DTA	desired time of arrival
GPS	global positioning satellite
ITS	intelligent transportation system
mph	miles per hour
O-D	origin-destination pair
PDF	probability density function
PeMS	performance measurement system
PMF	probability mass function
RMS	root mean square (of a set of values)
SSD	semi-standard deviation
TMC	transportation management center
TTI	travel time index
V2V	vehicle-to-vehicle (variations in travel times)
V/C	ratio of volume (or, more appropriately, demand) to capacity
VMT	vehicle-miles traveled

Terms

buffer index: Computed as the difference between the 95th percentile travel time and the average travel time, normalized by the average travel time.

distribution: The relative frequency with which a variable takes on specific values or lies within specific ranges of values.

failure/on-time measure: Computed as the percent of trips with travel times less than a threshold (Calibrated Factor [e.g., 1.3] * Mean Travel Time).

Harvey Balls: A technique for displaying information in which the variable's value is characterized by the extent to which a circle is filled, as in .

histogram: A graphical portrayal of the manner in which the values for a specific variable are distributed, typically on the basis of a set of bins (value ranges) into which the observations are placed.

misery index: Computed as the difference between the average of the travel times for the 0.5–5-percent longest trips and the average travel time, normalized by the average travel time (useful primarily for rural conditions).

nonrecurring event: An event that does not occur regularly during a typical time of day, including traffic incidents, work zones, weather, special events, traffic control devices, and fluctuations in demand. The effect of nonrecurring events can be magnified by inadequate base capacity.

planning time index: Computed as the 95th percentile travel time index divided by the free-flow travel time.

probability density function: a function that describes the relative likelihood that a continuous random variable will take on a given value. PDF values are not probabilities as such; a PDF must be integrated over an interval to yield a probability.

probability mass function: a function that describes the relative likelihood that a discrete random variable is exactly equal to some value.

regime: A specific condition under which a segment, route, or network is operating at a given point in time. It is effectively the "loading condition" for the system at that point in time. An example would be heavy congestion in conjunction with an incident.

root mean square delay: The square root of the mean of the squares of the delay values given some reference value that constitutes no delay.

route: A sequence of segments.

sample space: The set of raw data that pertain to each context for which a probability density function is being developed, such as those that pertain to a regime (e.g., congested conditions) or to another logical grouping (e.g., 7:00–9:00 a.m.) Also known as an observation set, observation time frame, or sample frame.

segment: A path between two locations on a network, preferably between the midpoints of the links.

semi-standard deviation: The square root of the sum of the deviations of observed values above (or below) a reference value.

skew statistic: Computed as the ratio of (90th percentile travel time minus the median) divided by (the median minus the 10th percentile).

travel rate: Travel time per unit distance.

travel time: The amount of time spent traveling over a given segment or route.

travel time index: A specific value of travel time divided by a reference value as in the free-flow travel time.

trip time: The door-to-door time for a trip.

user: People or package making a trip across the network.

Introduction

Reliability is a topic of great interest today. With the impacts of congestion, incidents, and other unforeseen circumstances, people are concerned about being able to get to work on time, catch flights, get to doctor's appointments, get children to and from day-care centers, and other events where being on time matters. Shippers are concerned that deliveries need to be on time, or penalties may be incurred and production processes may be disrupted. If the transportation system was 100% reliable, with the same travel times all the time, none of this would be an issue. But such is not the case.

Reliability information is desired by various audiences in different ways. Those with an interest in information range from decision makers, operators, and developers of reliability monitoring systems, to road users and shippers. For example, travelers and shippers want to know when they need to leave, or when the truck has to depart, in order to make an on-time arrival. Both groups also want to know what paths they should use to minimize the likelihood of encountering unforeseeable delays. Managing agencies want to know where the problem spots lie; where the network segments are that make the travel times vary.

This handbook offers numerous ideas on how to communicate reliability information in graphical and tabular form. It describes the display options listed in Table 1. The table shows the audiences to which they are likely to pertain. The display options fall into categories of maps, tables, and figures and graphs.

The handbook is intended to be used both as a supplement to the L02 materials and as a stand-alone reference. In light of the stand-alone objective, some redundancy exists with the L02 materials. Readers familiar with the L02 materials can skip over the redundant discussions; but for those who use this as a stand-alone reference, all of the material will be useful.

Table 1. Display Options and Their Audiences

	Audiences				
Type of Display	Users*	Decision-Makers	Policy Analysts	Operations Managers	System Analysts
Maps					
Graphic Icons (e.g., Harvey Balls)	X	X	s	s	X
Color Coded Links	X	X	s	s	X
Speed Contour Plots			s	X	X
Tables					
Reliability by Link	s			X	X
Reliability by Regime			X	X	X
Figures and Graphs					
Cumulative Distribution Functions		s	X	X	X
Probability Density Functions		s	X	X	X
Pie Charts		X	X	X	X

* Motorists, shippers, drivers, etc.

Key
X: very likely to use
s: will use sometimes

The text that follows offers numerous ideas on how to communicate reliability information in graphical and tabular form. It endeavors to meet the needs of all these audiences, ranging from novices to experts, from those for whom reliability is of cursory interest to those who want to understand all of the details and nuances. This means that some of the presentation ideas are very simple, while others are more complex. Each is intended to be clear about what reliability information is being presented and how it should be interpreted.

Insofar as the map-based displays are concerned, graphic icons like Harvey Balls provide a way to communicate reliability information in the same way that people see ratings of restaurants, consumer products, and other items (see Wikipedia, 2014). Maps that use color-coded links show the same information, but in a different format. Speed contour plots show variations in speeds by location and by time of day (through time-space diagrams or animations). The maps that use graphic icons and color coding will likely be used heavily by users and decision makers, because they present a high-level view in a succinct manner. The speed contour plots will be used by operations managers and system analysts, who can see patterns in performance by reviewing them.

To show a simple map example, it is useful to draw on people's prior experience with ratings displays used to depict the performance of consumer items, restaurants, and other items. Figure 1 uses graphic icons to indicate the reliability of links in the network. The more colored boxes there are, the poorer is the reliability.

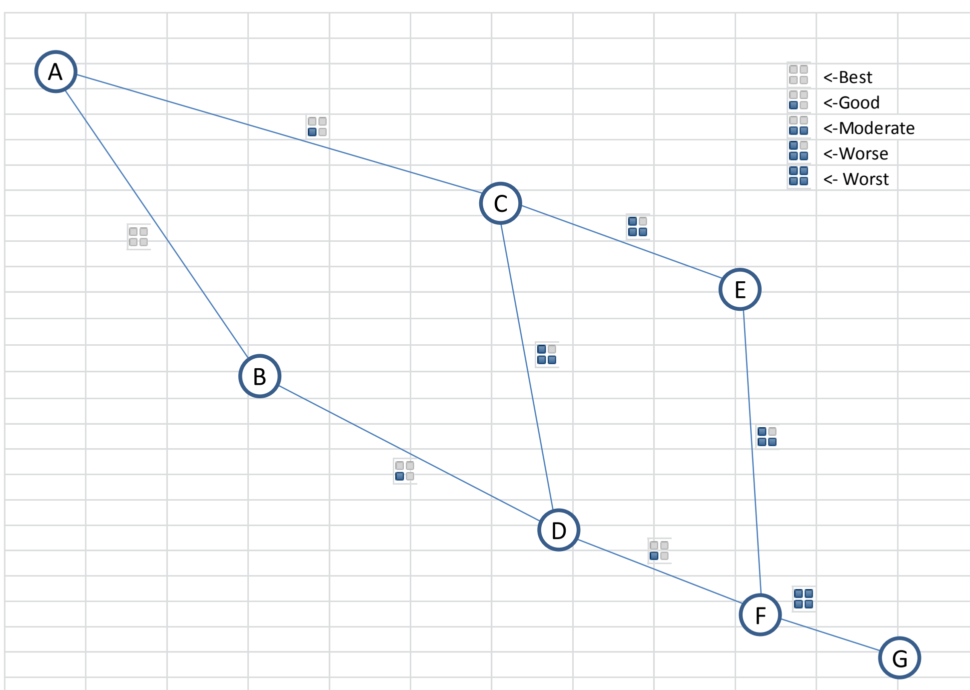

Figure 1. A simple reliability display.

It is easy to see that the path from A to G via A-B-D-F-G is the most reliable. It has the most links with good reliability and one with the best. Path A-C-D-F-G is clearly not as good, although it is not as bad as A-C-E-F-G. To a traveler or a shipper, this might be enough information for making a path choice decision. And if the icons were reviewed over time, as in an animation, the display could help the user select a departure time as well.

Tables of reliability information show metrics by link, network, or regime; that is, operating conditions. These displays are most likely to be used by operations managers, system analysts, and to a lesser extent by policy analysts. This information is most meaningful to individuals engaged in quantitative analyses.

Without becoming engaged in the details, which will be presented later, an example table display is shown in Table 2. It gives a sense of how the system is operating. Bigger values for the frequency of occurrence means the condition exists more often. Bigger values for the root mean square (RMS) delay mean that reliability is worse. It is easy to see that a condition like (uncongested, normal) occurs a lot, and its reliability is good. On the other hand, a condition like (congested, weather) does not occur frequently, but when it occurs, its reliability is poor.

Table 2. Table Portraying Reliability Information

1	2	3	4	5	6	7	8	9	10	11
CongCond	NRecCond	nObs	AvgRte	SD(Rte)	AvgInc	RmsDly*	SSD*	SemiVar*	Severity	RelSev
High	Demand	458	85.9	9.4	7.5	10.02	10.67	113.76	4588	14.0
High	Incidents	447	88.0	17.1	12.0	17.51	21.70	470.81	7826	23.9
High	Normal	10855	61.6	8.8	0.2	1.31	6.75	45.60	14211	43.4
High	Special Events	95	83.1	16.7	8.9	15.56	22.61	511.38	1479	4.5
High	Weather	149	95.2	27.8	19.9	31.06	38.10	1451.54	4627	14.1
Total		12004	n/a	n/a	n/a	n/a	n/a	n/a	32730.99	100.0
	* Note: 5-th percentile travel rate used for SSD =				80.0		sec/mi			

Figures and graphs present detailed information about the performance of individual segments or routes. They provide ways to study the reliability of facilities under different operating conditions and at different points in time. These displays are principally used by system operators and analysts, although decision makers and policy makers sometimes make use of them also. A good example of a figure can be seen in Figure 2.

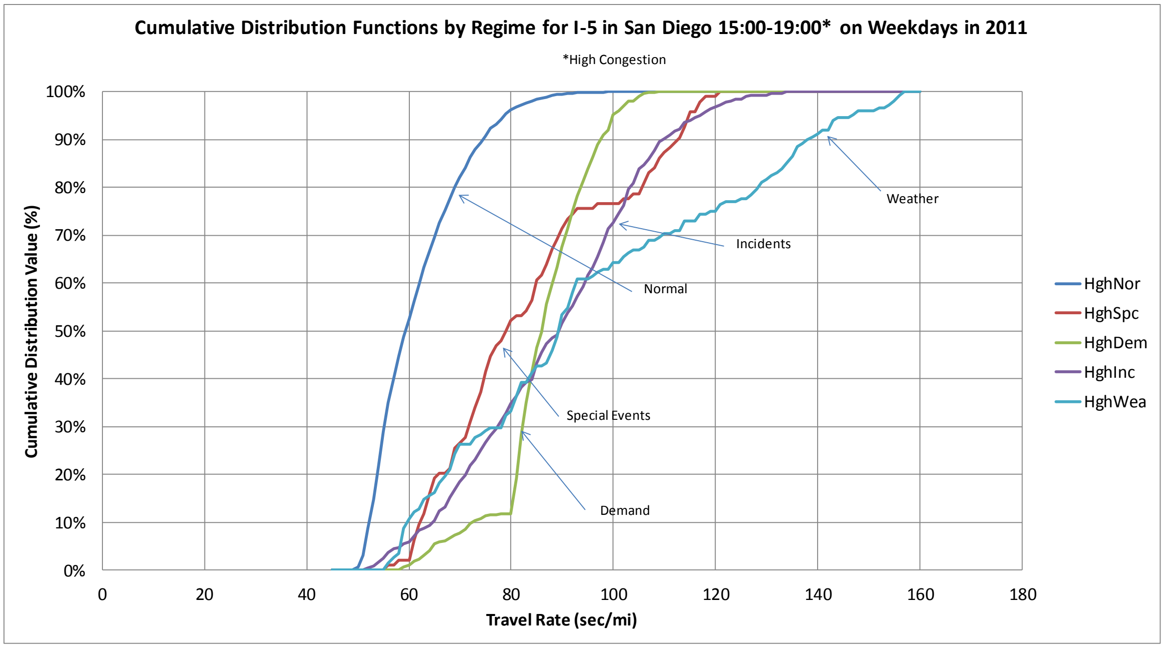

Figure 2. A graphic portrayal of reliability for various operating conditions.

Again, without becoming involved with the details, which will be discussed later, the distribution of travel times is shown for a variety of operating conditions. In this instance, distributions that are farther to the left and more vertical are better. It is again easy to see that the reliability of (uncongested, normal) is quite good while the reliability of (congested, incidents) is much poorer.

Travel Time Reliability

When reliability engineers think in terms of unreliability, they think of the probability of failure, failure modes, failure analysis, the mean time between failures, and strategies to improve these metrics including preventative maintenance and redundancy.

These ideas are not the sense of reliability being used in highway performance studies. Rather, highway system assessments tend to focus on the probability that specific travel times or travel rates can be achieved under specific operating conditions.

Reliability was originally defined by Ebeling (1997) as “the probability that a component or system will perform a required function for a given period of time when used under stated operating conditions. It is the probability of a non-failure over time.” This is slightly different from the idea of consistency, which has to do with the absence of variability.

Were Ebeling’s ideas to be applied in a transportation network context, the focus would be on individual trips and the system would be deemed reliable if each traveler or shipper experienced actual times of arrival (ATAs) that matched desired times of arrival (DTAs) within some window, as shown in Figure 3.

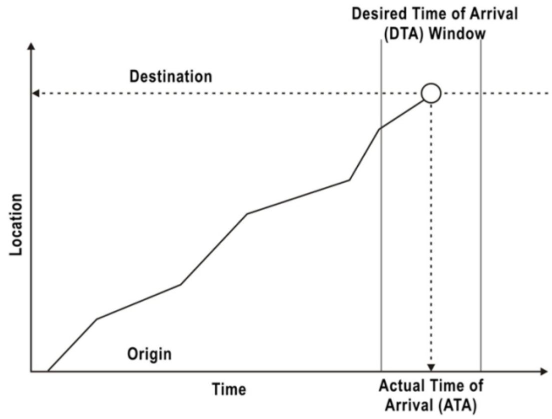

(a) DTAs and ATAs

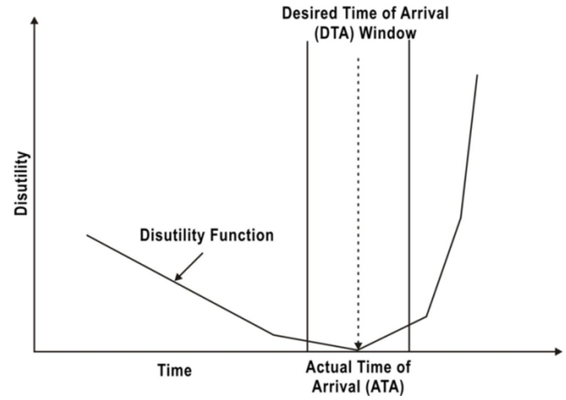

(b) Disutility based on the ATA

Figure 3. Highway reliability concepts consistent with reliability theory: desired times of arrival (DTAs), actual times of arrival (ATAs), and disutility.

Consistent with Ebeling's reliability theory, the "cost" of arriving within the DTA window would be 0, and it would be infinite outside that window (i.e., treated as a failure). Reliability would be measured in terms of the probability that the ATA was within the DTA window.

Within the context of transportation, it would be possible to interpret this cost as the disutility of missing the DTA. A dead zone could exist where the disutility is 0 (e.g., between 10 minutes early and 5 minutes late) and then there could be increases in disutility—linear or nonlinear—as the difference between the ATA and the DTA grows. Moreover, the disutility of being early could be different from that of being late.

If vehicles equipped with automated vehicle location (AVL) were prevalent and DTA windows were recorded for trips, it would be possible to assess the system reliability on the basis of the percent of ATAs that fall within their DTA windows. This would be a useful metric both for the entities making the trips as well as the organizations providing the service (e.g., the transportation management center (TMC) or transit system operator). The aggregate disutility could also be computed by summing the disutility values for each trip.

Obviously, this trip-level world of observability does not presently exist. What can be observed, at least for some vehicles, are travel times on segments and routes. Many urban areas can monitor toll tags or Bluetooth-equipped devices. Without either of these, agencies can estimate travel times from speeds observed at locations where field sensors (e.g., loops) are installed or obtain data from private vendors based on their subscribed fleets of instrumented vehicles.

In a highway context, the most common way to think about travel time reliability is the absence of variability in the travel times. This is akin to but not the same as examining the variance or standard deviation. A system is reliable if long travel times occur infrequently. Such assessments are most often done in the context of a system's ability to provide reliable average travel times for a specific time of day and/or operating condition (e.g., the a.m. peak hour on weekdays). Notions of reliability can also be examined in the context of individual vehicle or trip travel times. But this is uncommon today. The first of these assessments is effectively focused on day-to-day (D2D) variability; the second addresses vehicle-to-vehicle (V2V) variability. And the second can be used to examine D2D variability. The L02 project studied all of these.

Basic Displays

Since highway reliability focuses on the variability in vehicle, person, or package travel times (and rates), the basic displays of reliability information involve histograms, cumulative histograms, probability density functions (PDFs), probability mass functions (PMFs), and cumulative distribution functions (CDFs). The term *probability mass function* pertains when the observations are discrete, and *probability density function* pertains when the distribution is continuous, as is the case for a normal distribution. For purposes of clarity in this document, *probability mass function* is used because all the distributions are discrete, along with the acronym *PMF*, even though *PDF* is the more common term. The observations have often been binned, so the distribution appears to be discrete rather than continuous.

Figure 4 illustrates each of these basic ways to display reliability information. Assume there is a hypothetical freeway with a free-flow speed of 70 mph. This is equivalent to a free-flow travel rate of about 50 sec/mi. Assume the travel rates across some segment have been observed within a peak hour for 200 vehicles, and the observations have been binned into 1-sec/mi bins. The distributions being displayed are probability mass functions because the underlying observations have been placed into discrete bins.

Part (a) shows the histogram for these data. Each bar indicates how many vehicles have been observed with a travel rate falling in a specific 1-sec/mi bin. As can be seen, most of the vehicles have travel rates between 50 and 65 sec/mi.

Part (b) shows the cumulative histogram. Each bar indicates how many vehicles have observed travel rates equal to or less than a specific value. For example, 100 vehicles have been observed with travel rates less than or equal to 60 sec/mi; half of the total observations. All of the vehicles have travel rates less than or equal to about 100 sec/mi.

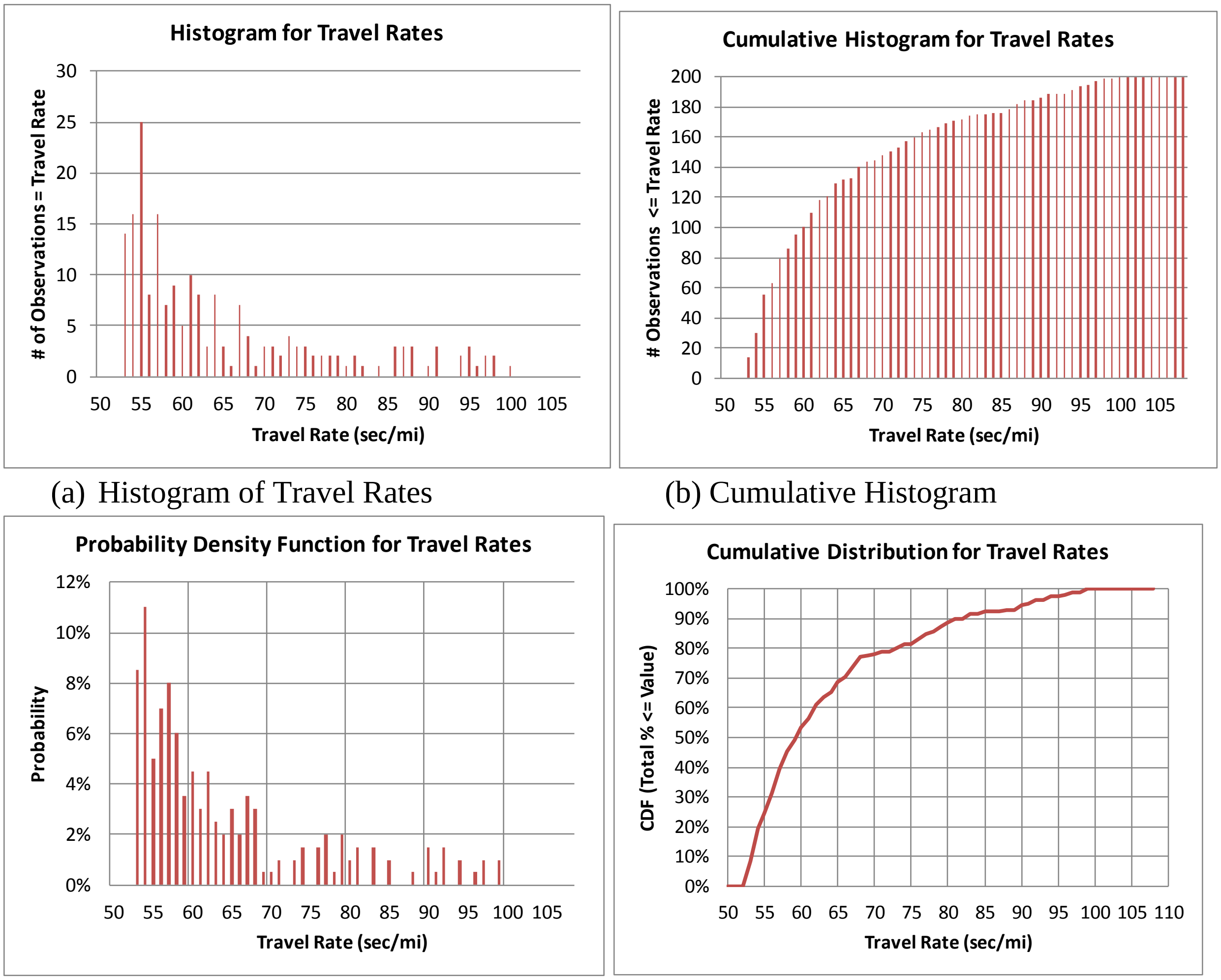

(a) Histogram of Travel Rates

(b) Cumulative Histogram

(c) Probability Mass Function

(d) Cumulative Distribution Function

Figure 4. Basic displays of reliability information.

Part (c) shows the probability mass function for these same data. The significant change is that the total of the bar heights is equal to 1.0 (i.e., 100%). Each of the values shown in Part (a) has been divided by 200, the total number of vehicles observed, to compute the probability that a vehicle has a travel rate equal to a specific value. In this instance a probability mass function is involved, rather than a probability density function, because the binned data are discrete counts, being based on the binning shown in Part (a). The probabilities can be interpreted as percentages. For example, 0.1 implies 10% or a 10% probability of being that specific value.

Part (d) presents the cumulative distribution function for the observed data. As with the probability mass function, all of the values shown in Part (b) are divided by 200. This makes the total percentage of observations reach a maximum of 1.0 (i.e., 100%).

In reliability analyses, the histograms are very valuable when the focus is on the number of times a particular average travel rate is observed, depending on the operating condition. To illustrate, assume that a freeway operates in one of two regimes during the peak hour: recurring congestion or nonrecurring congestion. Moreover, assume that on two out of every three days it operates in the recurring congestion regime and on the other day it is in the nonrecurring congestion regime. Now imagine that 300 peak-hour average travel time observations have been collected (perhaps for 300 consecutive peak hours) and that these travel times have been converted into rates (sec/mi). From what has been said above, 200 of these observations will fall into the recurring congestion category and the other 100 will be in the nonrecurring condition.

Figure 5 presents a set of graphs that depict the travel rate performance of this freeway for the 300 peak hours. Compared with Figure 2, here the focus is on day-to-day variations in the average rates, not variations in the vehicle-to-vehicle rates.

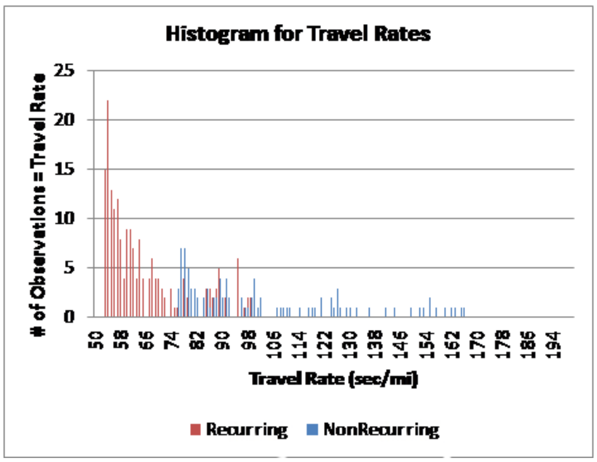

(a) Histogram for Travel Rates

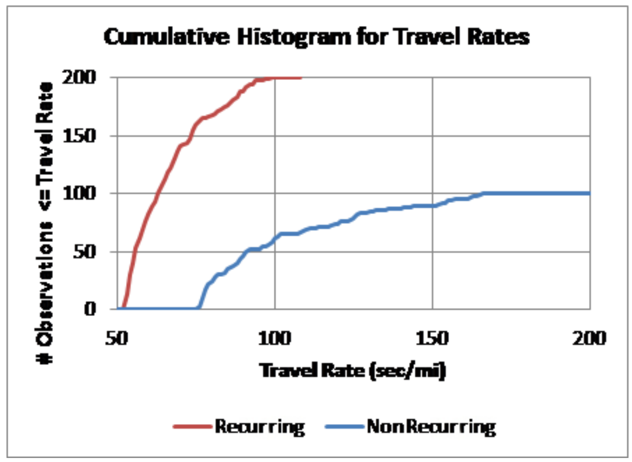

(b) Cumulative Histogram

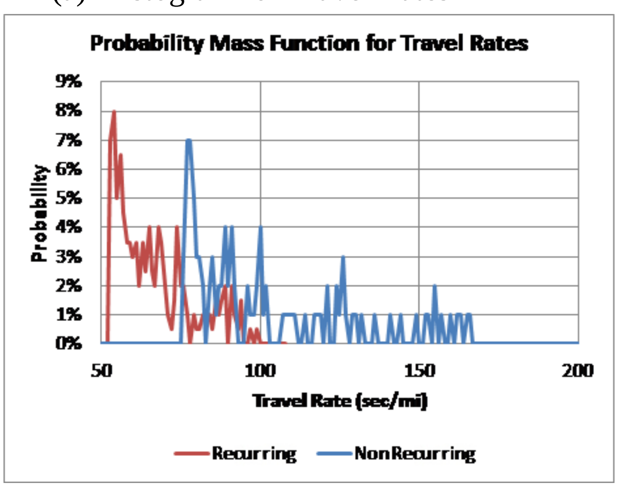

(c) Probability Mass Function

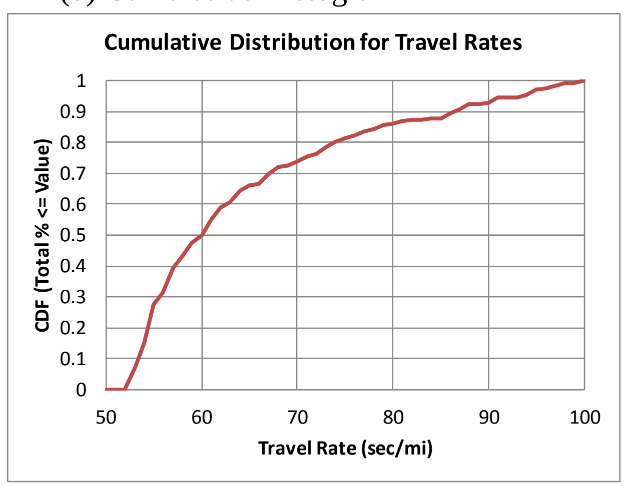

(d) Cumulative Distribution Function

Figure 5. Basic displays of reliability information for a multiregime situation.

Part (a) shows the histogram of the travel rates for the two operating conditions. The data for the recurring condition are shown in red; the nonrecurring data are shown in blue. It is easy to see that the travel rates for the nonrecurring condition are greater than those for the recurring condition. It is also easy to see, by the heights of the bars, that the recurring condition occurs more frequently than the nonrecurring condition.

Part (b) shows the corresponding cumulative histograms. As with Part (a), this plot shows the distribution of the travel rates for the two conditions and the relative frequency with which the conditions occur (200 versus 100).

Part (c) shows the probability mass functions for the two operating conditions. Notice how this graph is different from the one presented in Part (a). The data for each condition in Part (a) have been divided by the respective total observations (200 or 100). Because of this, probabilities have been computed indicating the likelihood that specific travel rates will occur under the two operating conditions. The information about the relative occurrence of these two conditions is not displayed. On the other hand, because they have been normalized, it is possible to compare the probability mass functions for the two operating regimes.

Part (d) shows the cumulative distribution function for the individual operating conditions. The data from Part (b) have been divided by the respective total observations (200 or 100) to compute cumulative probabilities that the travel rate will be less than or equal to a specific value. As with Part (c), the information about the relative frequency of occurrence for these two conditions is not displayed. But it is possible to compare the two cumulative distributions because they have been normalized to have a maximum value of 1.0.

Four additional displays of this information are possible when stacked plots are employed. They are depicted in Figure 6.

Part (a) shows a stacked-bar chart histogram. The observations of the nonrecurring congestion have been stacked on top of those for the recurring congestion condition so that the overall histogram can be seen (the cumulative heights of the bars) as well as the distribution of the values for the recurring and nonrecurring conditions. As with the Part (a) graph in Figure 3, it is possible to see that the travel rates for the recurring congestion condition are less than those for the nonrecurring condition, and in mid-range it is possible to see the relative occurrence of specific travel rates between the two regimes.

Part (b) shows the cumulative histograms stacked one on top of the other. Here it is easy to see that the total reaches 300. It is also easy to see that the recurring congestion contributes most if not all of the observations up to about 70; the nonrecurring congestion condition contributes all of the observations above 100 sec/mi; and in between, both conditions contribute observations.

Parts (c) and (d) show similar probability mass functions and cumulative distributions for the two regimes combined. In this case, the total of the probabilities for the two regimes combined totals to 1.0, so, unlike the graphs in Parts (c) and (d) of Figure 3, the relative contributions can be seen for the two regimes as they combine to form the overall PMF and CDF. As pointed out by Tu et al. (2008), these PMFs and CDFs represent sufficient information to answer the questions about measuring reliability.

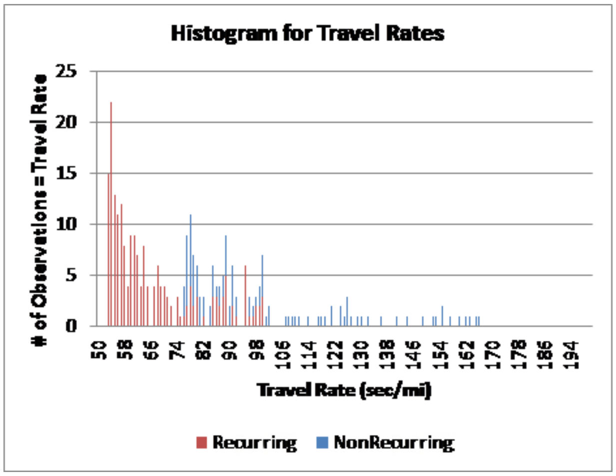

(a) Histogram for Travel Rates

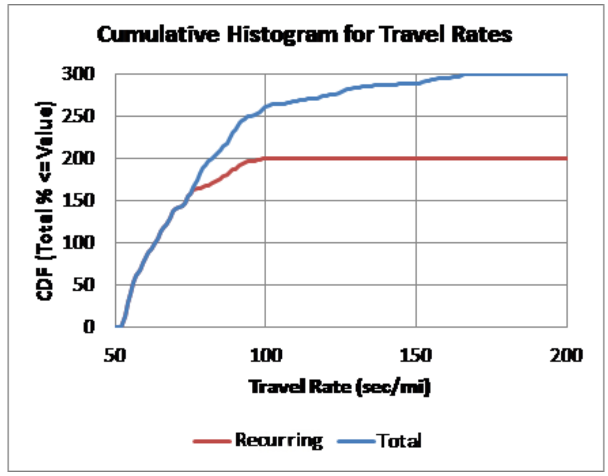

(b) Cumulative Histogram

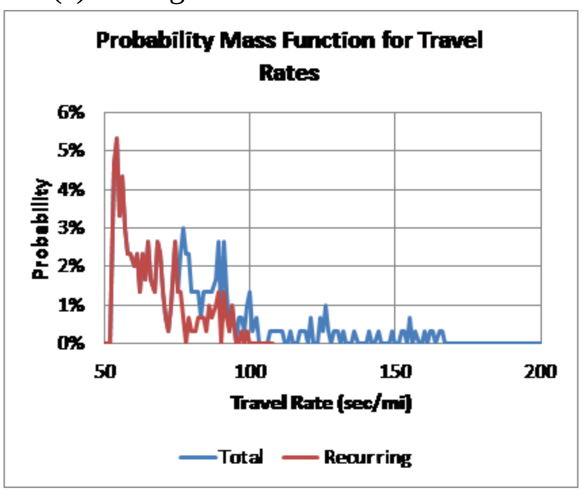

(c) Probability Mass Function

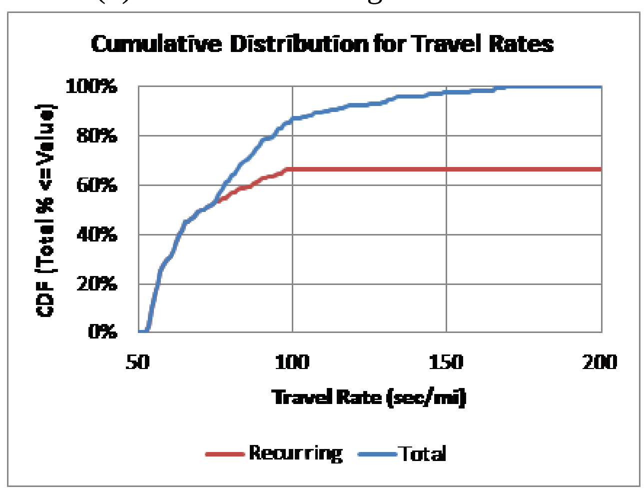

(d) Cumulative Distribution Function

Figure 6. Other displays of reliability information for a multiregime situation.

Single Value Reliability Measures

It is very useful to have a simple metric that summarizes the reliability performance shown in the PMFs and CDFs. A statistician might immediately focus on the mean, the variance, and a specific percentile. Many reliability measures have been suggested. An important point to keep in mind is that all of these metrics are derived from the PMFs and CDFs described earlier. Some of the common reliability measures (see http://ops.fhwa.dot.gov/publications/tt_reliability/ for example) are

- Buffer index: Computed as the difference between the 95th percentile travel time and the average travel time, normalized by the average travel time.
- Planning time index: Computed as the 95th percentile travel time index divided by the free-flow travel time.

- Skew statistic: Computed as the ratio of (90th percentile travel time minus the median) divided by (the median minus the 10th percentile).
- Misery index: Computed as the difference between the average of the travel times for the (0.5–5) percent longest trips and the average travel time, normalized by the average travel time (useful primarily for rural conditions).
- Failure/on-time measure: Computed as the percent of trips with travel times less than a threshold (Calibrated Factor (e.g., 1.3) * mean travel time).

The use of a metric called the semi-standard deviation (SSD) was suggested by L02. It is the square root of the semi-variance. Technically, the SSD σ_r is the square root of the sum of the deviations of the observed travel times t_i above a reference travel time t_r (or in the case of rates, the deviations of the observed travel rates τ_i above a reference travel rate τ_r). The SSD is frequently used in risk analysis to assess the extent that risk exposure will exceed a given threshold.

The SSD bases its value on the observations t_i that are greater than or equal to t_r (count = n_r):

$$SSD_r = \sqrt{\frac{1}{n_r}\sum_{i=1}^{n}\left(t_i - t_r\right)^2} \quad \exists\, t_i \geq t_r \tag{1}$$

A very closely related metric is the root mean square (RMS) delay $\tilde{d}_r$. $\tilde{d}_r$ is based on the same reference value t_r as the SSD (or the RMS delay per mile $\hat{\delta}_r$ given a reference value τ_r) but $\tilde{d}_r$ includes a term for each of the observations, not just those above the reference value. And the delays for the travel times less than the reference value are set to 0. Hence, if the travel time observations are t_i and the reference value is t_r , then $\tilde{d}_r$ is computed as follows:

$$\tilde{d}_r = \sqrt{\frac{1}{n}\sum_{i=1}^{n}\left(\Delta t_{ir}\right)^2} \qquad where \quad \Delta t_{ir} = \max(t_i - t_r, 0)\ \forall\, i \tag{2}$$

If the RMS delays are measured per mile as in τ_i, the equation is the same, but the travel rates are used instead of the travel times:

$$\tilde{\delta}_r = \sqrt{\frac{1}{n}\sum_{i=1}^{n}\left(\Delta \tau_{ir}\right)^2} \qquad where \quad \Delta \tau_{ir} = \max(\tau_i - \tau_r, 0)\ \forall\, i \tag{3}$$

Because $\tilde{d}_r$ and $\tilde{\delta}_r$ use all of the observations, they are sensitive to the entire distribution of delays.

To illustrate the computation of $\tilde{d}_r$, assume that a specific facility has a free-flow travel time of 5 minutes. Further, assume that a reference travel time of 7 minutes (higher than the free-flow travel time) is being used by the agency to assess travel time reliability. Given this reference value, all of the observations above 7 minutes represent unreliable operation, and those below do not, even though they are greater than or equal to the free-flow travel time. Now assume that the travel times observed for seven vehicles during a nonrecurring event are 6, 5, 6, 7, 9, 10, and 11. In computing $\tilde{d}_r$ for this condition, the first three observations (6, 5, and 6) are set to 0, because they have travel times less than the reference. $\tilde{d}_r$ would be computed as follows:

$$\tilde{d}_r = \sqrt{\frac{1}{7}\left[(0)^2 + (0)^2 + (0)^2 + (0)^2 + (2)^2 + (3)^2 + (4)^2\right]} \qquad (4)$$

Numerically, the result is that $\tilde{d}_r$ = 2.04.

To study this calculation a little more, $\Delta t_{ir} = \max(t_i - t_r, 0)$ can be computed for each t_i as shown above. These are the differences between the observed travel times t_i and the reference value t_r. $\tilde{d}_r$ is the square root of the average of these $(\Delta t_{ir})^2$ values. In contrast, the average delay $\bar{d}_r$ is the arithmetic average of the Δt_{ir} values. Numerically, $\bar{d}_r$ = 1.29 = $^1/_7$(0 + 0 + 0 + 0 + 2 + 3 + 4). Because $\tilde{d}_r$ squares the differences before adding them and taking the square root, it places more emphasis on the larger deviations.

Like the average delay or the traditional standard deviation σ, $\tilde{d}_r$ can be compared in magnitude with the reference value or other metrics like the mean. Larger $\tilde{d}_r$ values mean that the squares of the deviations are larger, so the performance can be seen as less reliable.

In terms of setting values for τ_r (and/or t_r), three possibilities are logical. One possibility is the travel rate implied by the free-flow speed. The other two possibilities are the travel rates implied by the posted speed limit (as is being done in North Carolina), or a policy-based acceptable speed (as in California).

Another metric that has received recent consideration is the "travel time index," or TTI. It is the ratio of a specific percentile travel time to the free-flow travel time. TTI values are often computed for the 50th percentile travel time (the median), the 80th percentile travel time, and the 95th percentile travel time. A display of these metrics and others is shown in Figure 7. Another measure, proposed by SHRP 2 Project C11 researchers, focuses on the cost of unreliability. That is, the dollar value of the delay caused by the difference in the 50th and 80th percentile TTI figures:

$$(VT) = TTI50+\alpha \times (TTI80-TTI50) \qquad (5)$$

$TTI_{e(VT)}$ is the TTI equivalent on the segment and α is the reliability ratio (the value of reliability divided by the value of time).

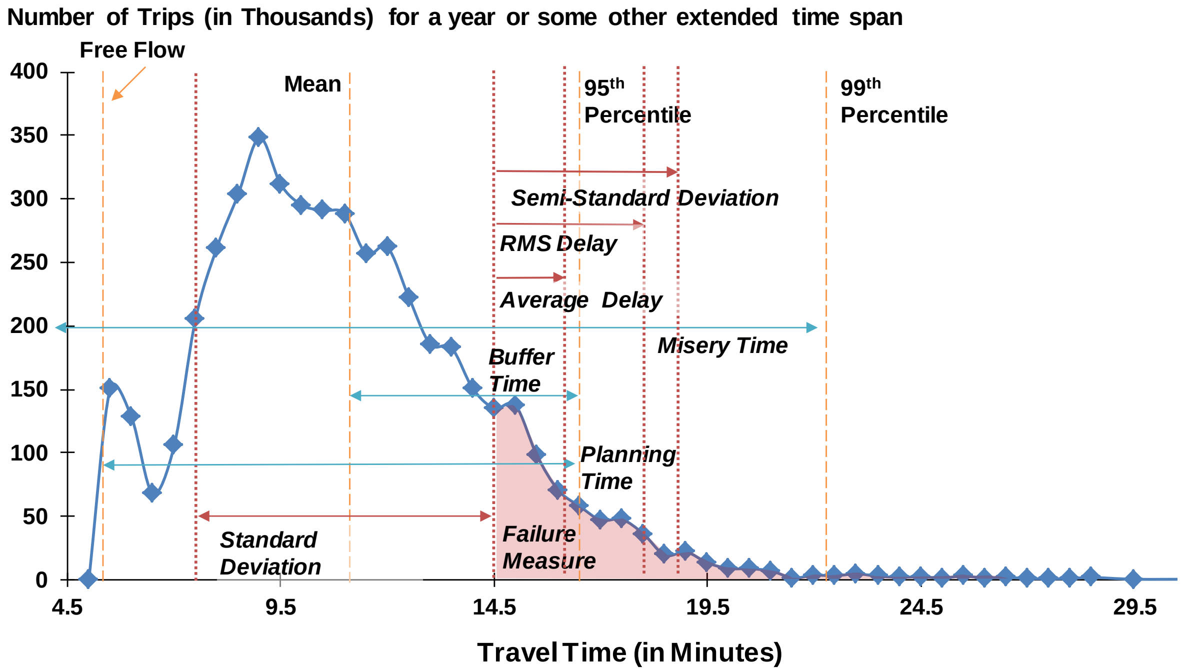

Source: Adapted from Zegeer et al. (2014).

Figure 7. A graphical illustration of reliability measures.

Many recent studies of the value of reliability (especially those in Europe) define the reliability ratio in terms of a single standard deviation in travel time. This is roughly equivalent to the difference in the 50th and 84th percentile TTI (assuming a one-tailed normal distribution).

Breakdowns by Regime

When doing reliability analysis, it is important to study the data in the context of regimes or operating conditions. Differences in the operating conditions will have a major impact on performance. This is the essence of the report for FHWA developed by Cambridge Systematics and Texas A&M Transportation Institute (2005) that talks about the “seven sources of congestion.” That study grouped the causes of congestion and unreliable travel times into three categories: (1) traffic influencing events (incidents, work zones, and weather), (2) traffic demand (fluctuations in normal traffic and special events), and (3) physical highway features (traffic control devices and bottlenecks). The point of that report was that congestion and system reliability are affected by the conditions under which the facility is operating. And seven categories seemed like a reasonable way to break down the operating conditions.

A problem with the “seven sources of congestion” notion is that data analysis based on those categories can miss the fact that reliability performance is actually affected by combinations of the nonrecurring event taking place, including none, and the traffic flow condition, that is, the congestion level. The importance of this bivariate classification was clearly evident to the L02 research. When congestion is high, work zones will have a far greater effect on reliability than they will when it is low. The same is true for weather.

This means it is important to think about reliability analysis in a two-dimensional way, with one dimension being the nonrecurring event taking place and the other being the level of congestion that would have been present if no nonrecurring event were taking place. In fact, a first cut of the data should be divided into normal and abnormal condition categories (i.e., normal and nonrecurring event categories), and then the data should be subdivided again on the basis of the level of congestion that would have been extant under normal conditions, effectively a reflection of the volume-to-capacity, V/C, ratio. In fact, the normal performance should be used as a benchmark against which to compare the nonrecurring event performance when endeavoring to measure or assess the impact of the nonrecurring events.

In the context of data processing, this means labeling every observation in two ways, whether it is for an individual vehicle or some aggregate of the vehicles (e.g., from a loop sensor). Otherwise, analysis of the variability (i.e., the reliability analysis) will be confounded by the variation caused by different operating conditions rather than the impact of variations in the specific operating condition and traffic behavior.

To re-emphasize, the first label should indicate the nonrecurring event that pertained at the time the observation was collected, including none. The second label should identify the nominal level of congestion (e.g., the V/C ratio) that would have pertained had there been no nonrecurring event (or the congestion level that did pertain if there were no nonrecurring event).

L02 used a two-dimensional matrix of regimes. An example is shown in Table 3. Each regime consisted of a nominal congestion level and a nonrecurring event condition. One example would be nominally moderate congestion in combination with a weather event, that is, cell (3, 2) in the matrix. The data falling into each of these cells would be analyzed for reliability performance, and the performance of the facility under one condition would be compared with another. Also, mixed observations can be given these category labels, and then the differences in performance under each condition can be seen.

The idea of a nominal level of congestion is perhaps uncommon, so an example helps. Imagine that a facility has been observed for some time and its operation under normal conditions has been documented. Consistent with standard traffic engineering practice, this results in an assessment of how the congestion level varies with the V/C ratio. That is, if conditions are normal, including the capacity, different demand flow rates result in different levels of congestion. This is the nominal congestion condition.

Consider an example. Imagine that a nonrecurring event has taken place. Labeling the observation based on the nonrecurring event should be the first step. It involves determining which nonrecurring event category pertains and adding that label. The second step is to determine what nominal congestion condition pertains. A way to do that is to take the arriving demand, say at flow rate *V* vehicles/hour, and compute a V/C ratio that would exist if no nonrecurring event were under way. A breakdown of these V/C ratios into levels of congestion allows a nominal congestion condition label to be assigned based on the V/C ratio that was computed. If the V/C ratio represents "moderate congestion," then the correct regime for this condition is cell (3, 3) in Table 3. That is, moderate nominal congestion in combination with an incident.

Table 3. Classifying and Labeling Reliability Data by Operating Regime

Reliability Regimes						
	Nonrecurring Condition					
		Nonrecurring Events				
Nominal Congestion Condition	None	Weather	Incident	High Demand	Special Event	Work Zone
Uncongested						
Low						
Moderate						
High						

As indicated before, the advantage to categorizing the data in this manner is that all of the observations within a given regime will reflect the facility's performance under the same operating conditions. That is, statistically valid information can be developed that indicates how the facility performs when the variance being observed is not due to significant variations in either the nominal level of congestion or the type of nonrecurring event. Rather, the variations are due to differences in the severity of the nonrecurring event and driver behavior.

To illustrate this process, assume that a set of travel time observations (or rates) have been placed in chronological order and that additional time-referenced databases exist for the traffic flow rates and nonrecurring event information. Assume these databases are synchronized in time. The labeling process can begin by finding a starting point where the operating condition is known. That condition is then labeled (e.g., uncongested with no nonrecurring event under way). The next step involves moving forward in time through the synchronized databases and adding the appropriate nonrecurring event label based on the event that was taking place, including "none." It is important to recognize that there might be a need to look at data in the opposite direction (i.e., rubbernecking) and on adjacent facilities (e.g., backup caused by a blocked exit ramp) to determine the correct nonrecurring event label. Then the appropriate congestion level label is added by looking at the traffic flow rate that was or would have been extant (under normal conditions) if no nonrecurring event were under way. This might be the traffic flow rate that would have normally existed at this point in time based on historical data and the traffic flow pattern leading up to this point in time. A very simple way to think about this is to use the common paradigm of a.m. peak, midday, p.m. peak, evening, late night, and early morning. These time-of-day labels track loosely to specific congestion levels. Of course, work days, day-of-the-week holidays, and so forth, are also important because these affect the nominal traffic flows as well.

Once the data have been labeled in this manner, the reliability analysis can proceed. The labels serve to categorize the observations, to differentiate among them in plots and tables, and to create summaries that indicate the relative reliability performance under the different regimes.

Displays that Highlight Regime Contrasts

Contrasts between the reliability of different regimes are often of interest. Here is an example based on 5-minute average travel times in 2011 for I-5 in San Diego, California, from the I-5-I-805 split south to 8th Street in National City. Each data point is a walk-the-matrix travel time for a 5-minute interval during the workdays. This totals to 72,000 observations.
Figure 8 is a display that helps immensely with being able to see when reliability is an issue (in this case on weekdays), just from normal traffic variations and when, at other times across the year there were variations due to unexpected (nonrecurring) events.

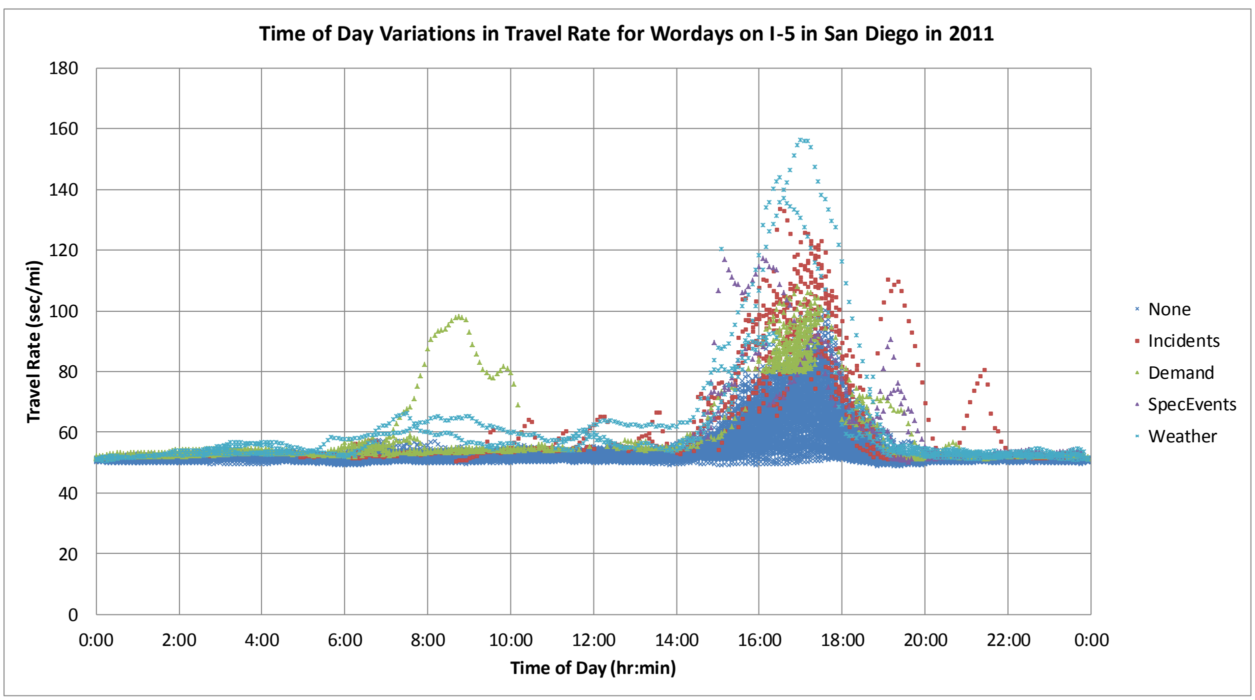

Figure 8. Variations in travel rates by time of day for weekdays, or workdays, in 2011.

To create the display, operating regime labels were added to the travel time (travel rate) observations. In this case, the original data were completely unlabeled. But it was clear that there had been nonrecurring events and that traffic volumes did have an impact even if no nonrecurring event was under way. The task was to determine what nonrecurring events did pertain to these observations and what the nominal congestion levels were, and then add the labels accordingly. For the nonrecurring events, historical databases were culled to look for evidence that events had occurred on specific days at specific times and locations. It proved important to look at data in both directions on the freeway and to search for evidence of events on intersecting freeways and major arterials. Fortunately, the network performance database, weather histories, and newspaper reports did make it possible to identify almost all of the nonrecurring events that had caused significant changes in travel times. For the nominal congestion levels, they were identified by looking at the variation in travel times by time of day that occurred on the normal days and then breaking the time of day down into different congestion levels. The breakpoints did not exactly line up with standard assumptions about when such time periods begin and end (e.g., the a.m. peak is from 7:00 to 9:00 a.m.). Rather, the data were used directly to determine these times of day. The nominal congestion level labeling is not explicitly shown in the figure, but the nominal congestion level labels were: uncongested conditions existed all day except from 14:15 to 18:50 when the condition was considered highly congested.

That the nominal level of congestion has an impact on reliability is easy to see if the travel times are plotted against vehicle-miles traveled (VMT)/hour/mile, as has been done in Figure 9.

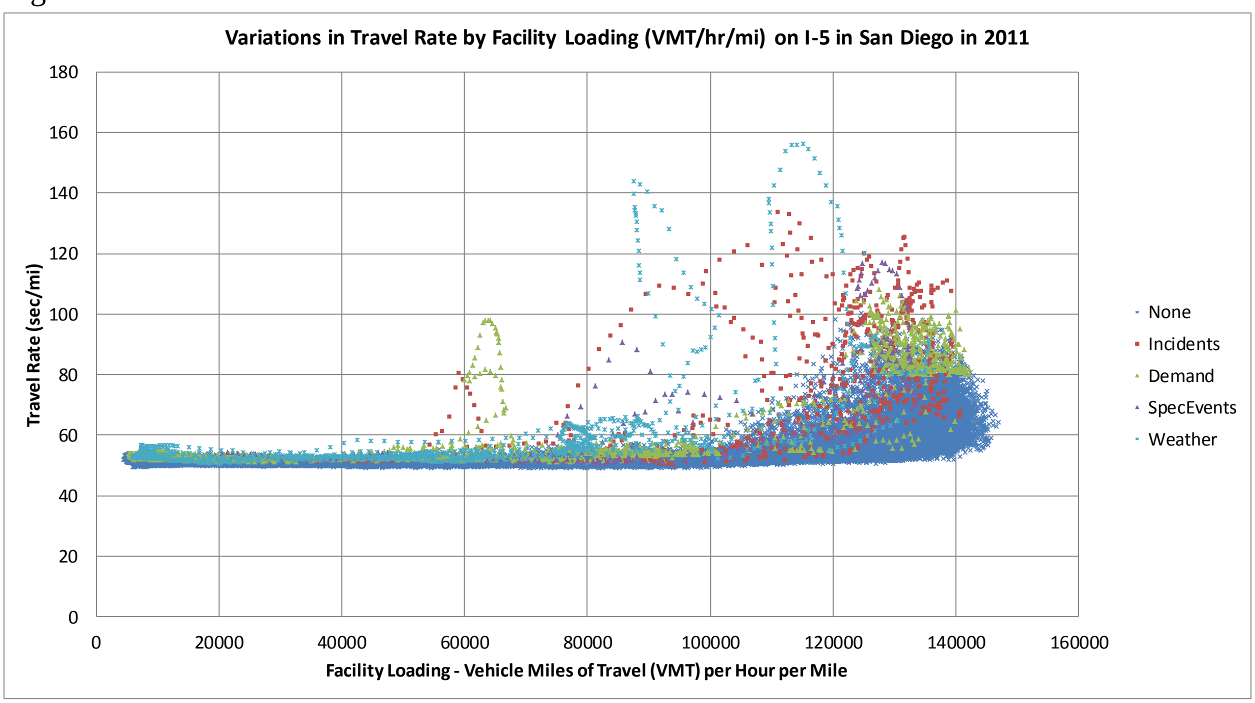

Figure 9. Variations in travel rates by time of day across a year.

From this display it is easy to see that when the facility loading is light, the travel rate is very consistent unless a nonrecurring event takes place. But, as the facility loading increases, the travel rate increases in general, and the variation in the travel rate grows as well. This display also makes it easy to see that nonrecurring events can create large travel rates at times when the facility loading would otherwise not have had a significant impact. (An example is the large travel rates that occurred because of extra demand and incidents for flow rates near 60,000 VMT/hour/mile.)

A partial listing of the breakdown of the 72,000 average 5-minute travel rate observations is shown in Table 4. In this display, each cell indicates the number of times that a specific travel rate was observed for a specific condition (one of 10) on this I-5-based route across the weekdays in 2011. Only a portion of the total observations are shown. The travel rates reach as high as 157 sec/mi for one observation in the regime of high congestion with weather.

This display makes it is easy to see that the uncongested/normal operating condition is the most common one. The cell values in the 50–60-sec/mi bins total more than 53,000. They represent 77% of the 72,000 travel rate observations. The last row of the table lists the total observations by operating regime. The uncongested/normal condition is the most common, followed by high congestion/normal, and then uncongested/high demand. These data can form the basis for PMFs, CDFs, pie charts, tables, and other types of displays.

Table 4. Breakdown of 5-Minute Travel Rate Observations by Operating Regime on I-5 in San Diego in 2011

TrvRate	HghNor	HghSpc	HghDem	HghInc	HghWea	UncNor	UncSpc	UncDem	UncInc	UncWea
45	0	0	0	0	0	0	0	0	0	0
46	0	0	0	0	0	0	0	0	0	0
47	0	0	0	0	0	0	0	0	0	0
48	0	0	0	0	0	0	0	0	0	0
49	1	0	0	0	0	3	0	0	0	0
50	54	0	0	0	0	880	0	0	0	0
51	288	0	0	0	0	19335	4	0	4	9
52	1048	0	0	1	0	23485	31	150	39	83
53	1043	0	0	1	0	6867	30	350	65	224
54	1195	0	0	3	0	4369	33	379	68	141
55	1128	0	1	5	1	490	8	210	23	84
56	778	0	3	4	1	50	3	60	12	49
57	656	0	2	5	4	28	0	28	15	51
58	564	2	3	2	5	12	1	16	3	26
59	455	1	5	5	9	4	1	7	9	21
60	421	1	4	3	5	8	0	3	4	27
61	401	5	2	6	1	2	4	2	6	14
62	358	4	2	6	3	0	1	0	3	14
63	400	2	4	3	3	0	0	2	2	23
64	373	4	5	5	4	0	1	0	3	14
65	317	3	6	7	4	0	1	0	3	9
66	332	2	3	9	4	0	0	1	3	6
67	280	1	1	6	3	0	3	2	3	2
68	266	1	3	9	3	0	1	4	0	0
69	252	4	3	7	5	0	0	3	0	0
70	235	1	3	10	3	0	1	0	1	0
71	211	1	3	6	1	0	0	2	1	0
72	235	4	6	13	1	0	2	2	0	0
73	183	3	2	7	2	0	1	0	0	0
74	149	4	2	9	1	0	3	0	1	0
75	162	4	3	8	2	0	1	0	0	0
76	165	3	1	6	2	0	0	2	1	0
77	95	3	0	7	1	0	1	0	2	0
78	111	1	1	7	0	0	0	1	0	0
79	117	2	0	7	4	0	0	2	1	0
80	102	2	0	9	2	0	0	3	0	0
81	62	1	34	7	6	0	0	2	1	0
82	39	0	42	8	4	0	1	2	0	0
83	56	1	30	5	0	0	0	1	1	0
84	40	2	30	3	4	0	0	1	0	0
85	38	4	23	15	2	0	1	0	0	0
86	28	1	15	10	0	0	0	1	0	0
Total	12783	104	472	466	175	55533	135	1250	285	797

To illustrate, Figure 10 shows the PMFs for these various operating conditions. The graph is somewhat hard to read because there are 10 PMFs displayed simultaneously. To help with this, three of the distributions have been highlighted: high congestion/special events, high congestion/extra demand, and uncongested/weather.

This display makes it easy to see that the regime that contributes to the highest travel rates is uncongested/weather. The graphs motivate thoughts about mitigating actions that might be taken to improve reliability. The display also highlights the high congestion/extra demand regime. Possibly, better information about travel conditions might mitigate the extra demand, and better demand management might help.

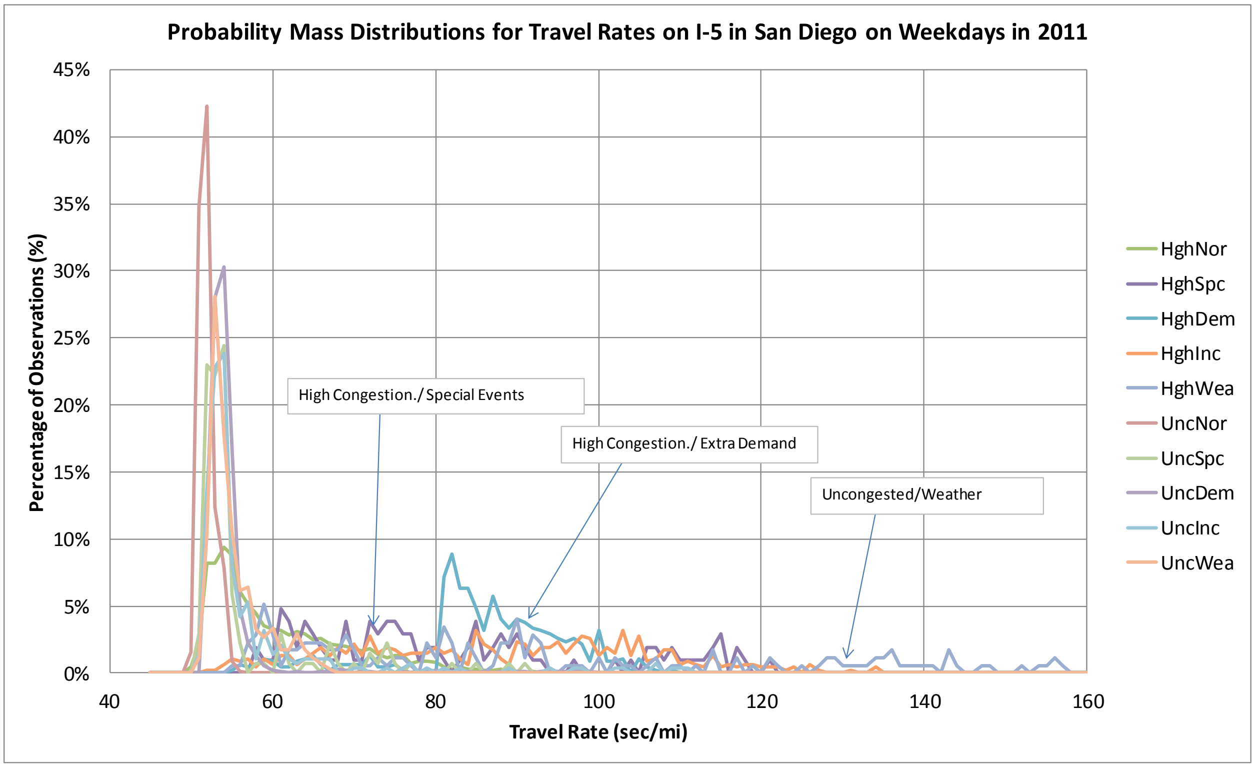

Figure 10. PMFs by regime for travel rates for weekdays on I-5 in San Diego in 2011.

Figure 11 shows the CDFs for these same ten operating conditions. This display makes it much easier easy to see that for many of the operating conditions, the travel rates are very consistent. This means the facility's operation can be deemed reliable under those conditions. But there are regimes for which this is not the case, like high congestion with incidents and high congestion with weather, which have been highlighted.

Displays of Reliability Assessments

This section focuses on displays that can be used to present the results of reliability assessments. The calculations are based on the ideas presented in the previous section. The displays primarily make use of the RMS delay. The displays would be similar if the other metrics were employed.

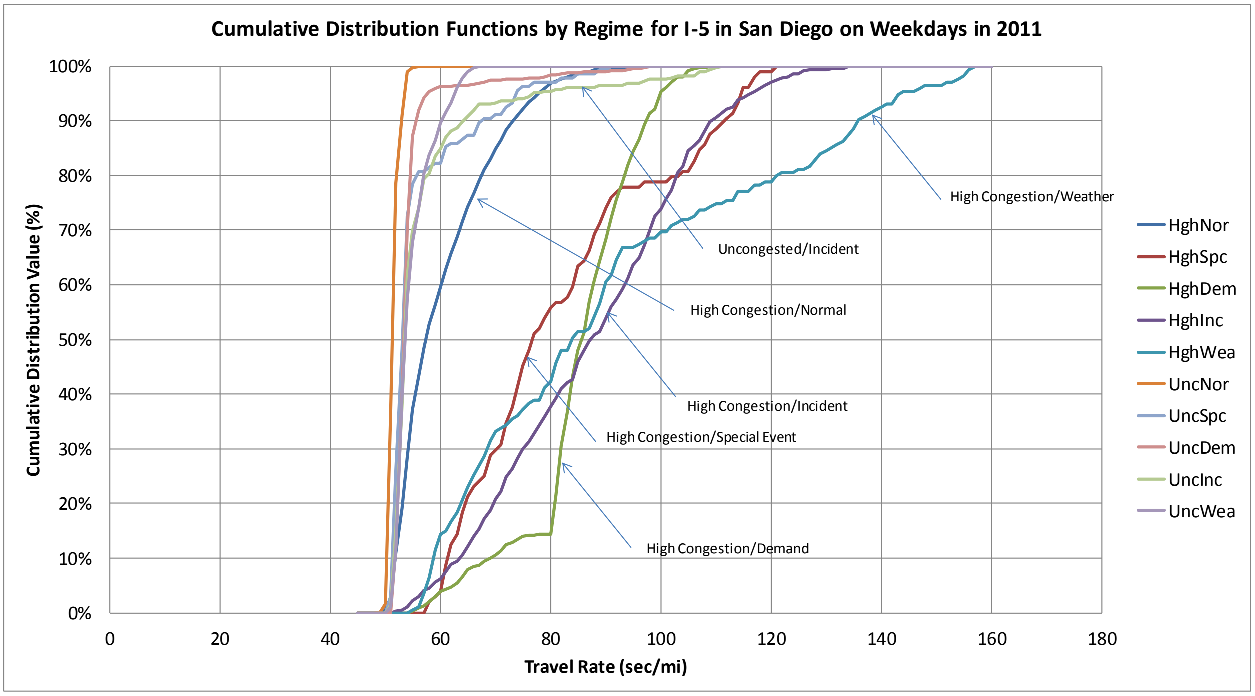

Figure 11. CDFs by regime for travel rates for weekdays on I-5 in San Diego in 2011.

Table 5 shows an assessment of $\tilde{\delta}_r$ for the ten operating conditions identified for I-5 in San Diego. The first two columns show the operating regime. Column 3 reports the number of 5-minute travel rate observations classified as belonging to each regime. Column 4 shows the average travel rate (sec/mi), Column 5 presents the standard deviation for those rates, Column 6 shows $\overline{\delta}_r$ based on the reference value of 50.4 sec/mi (in this case the 5th percentile travel rate), Column 7 shows $\tilde{\delta}_r$, Column 8 shows the SSD, and Column 9 presents the semi-variance on which the SSD is based. Column 10 is derived from the data in Columns 3 and 7. The number of observations for each regime have been multiplied by the SSD (like a vehicle-miles calculation) to create a metric that indicates in a sense the severity (significance) of each regime. Column 11 normalizes Column 10 based on the total.

Table 5. Reliability Assessment by Operating Regime for I-5 in San Diego in 2011

0	1	2	3	4	5	6	7	8	9	10	11
Label	CongCond	NRecCond	nObs	AvgRate	SD(Rate)	AvgDly	RmsDly*	SSD*	SemiVar*	Severity	RelSev
HghNor	High	Normal	12784	60.4	8.6	10.0	13.22	13.27	175.99	168957	53.6
HghDem	High	Demand	472	85.1	10.4	34.7	36.26	36.26	1314.51	17113	5.4
HghInc	High	Incidents	467	87.1	17.3	36.6	40.74	40.78	1663.14	19025	6.0
HghSpc	High	Special Events	105	81.7	16.8	31.2	35.99	36.17	1308.03	3779	1.2
HghWea	High	Weather	176	90.7	27.9	40.1	49.33	49.47	2447.31	8682	2.8
UncNor	Uncon	Normal	55534	51.5	1.0	1.1	1.44	1.48	2.20	79857	25.3
UncDem	Uncon	Demand	1251	54.4	5.0	4.0	6.83	6.83	46.68	8543	2.7
UncInc	Uncon	Incidents	286	56.9	9.9	6.5	12.28	12.30	151.36	3512	1.1
UncSpc	Uncon	Special Events	136	56.0	6.5	5.6	9.63	9.70	94.13	1310	0.4
UncWea	Uncon	Weather	798	54.8	2.7	4.5	5.58	5.59	31.21	4455	1.4
	Total		72009	n/a	n/a	n/a	n/a	n/a	n/a	315234	100.0
		* Note: 5-th percentile travel rate used for SSD =				50.4		sec/mi			

As can be seen from this display, any one of the metrics in Columns 4 through 8 could provide a sense of the variations in reliability among the regimes. For example, high congestion with a weather event always has the largest value. For the metric to be consistent with Figure 8, it should indicate that high congestion/weather is far more problematic than the next three conditions (high congestion/incident, high congestion/special, and high congestion/extra demand). The metrics for them should be very similar. The next most problematic condition should be high congestion/normal, and the next should be uncongested/incident, because of the long tail. $\tilde{\delta}_r$ is consistent with the anticipated assessment, and so are the other metrics to varying degrees.

The reader only has to look briefly at Table 5 to see that pie charts could be helpful in highlighting the contrasts in regime conditions. Figure 12 shows how frequently the various regimes occur and the reliability assessments associated with each.

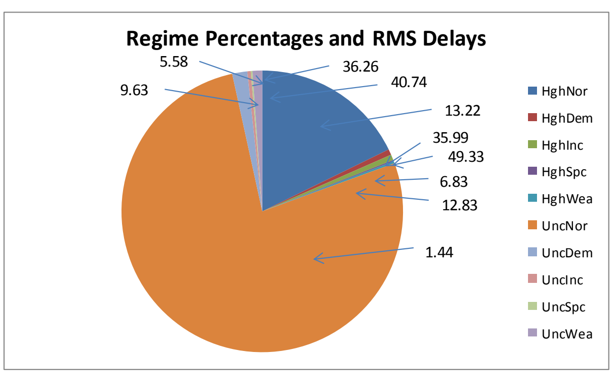

(a) All Regimes

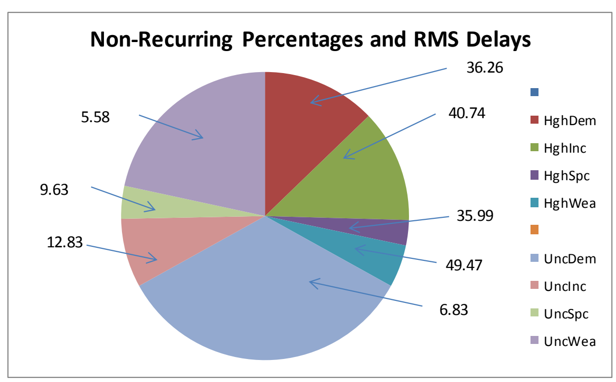

(b) Nonrecurring Event Regimes

Figure 12. Pie chart breakdowns of the operating regimes and reliability assessments for weekdays on I-5 in San Diego in 2011.

Part (a) shows the percentage of time during the year when all of the various regimes arise. The labels show the reliability assessments. It is easy to see that uncongested/normal is the most common regime and that congested/normal is the next most common. The much smaller percentages belong to the nonrecurring event conditions. Part (b) shows the distribution of the nonrecurring regimes. The normal regimes have been zeroed out. The display makes it easy to see that uncongested/demand and uncongested/weather together are the two dominant regimes representing more than half of the 5-minute nonrecurring event condition observations.

The graphs in Figure 12 would be even more useful if the heights of the pie slices could reflect the reliability performance. This is not a graphing option available in Excel, but it would be a useful one to develop as an add-in. Clearly, it is important to account for the significance of the unreliability in each of these conditions when evaluating mitigation strategies.

For the benefit of the readers of this handbook, and not necessarily intended as a display suggestion, Figure 13 presents a relative comparison of the four deviation-related metrics.

As can be seen, the metrics create different relative senses among the unreliability of the various regimes. The $\tilde{\delta}_r$ again seems very consistent with the anticipated assessment. (The SSD values lie behind the $\tilde{\delta}_r$ values, as would be anticipated by looking back to Table 5.)

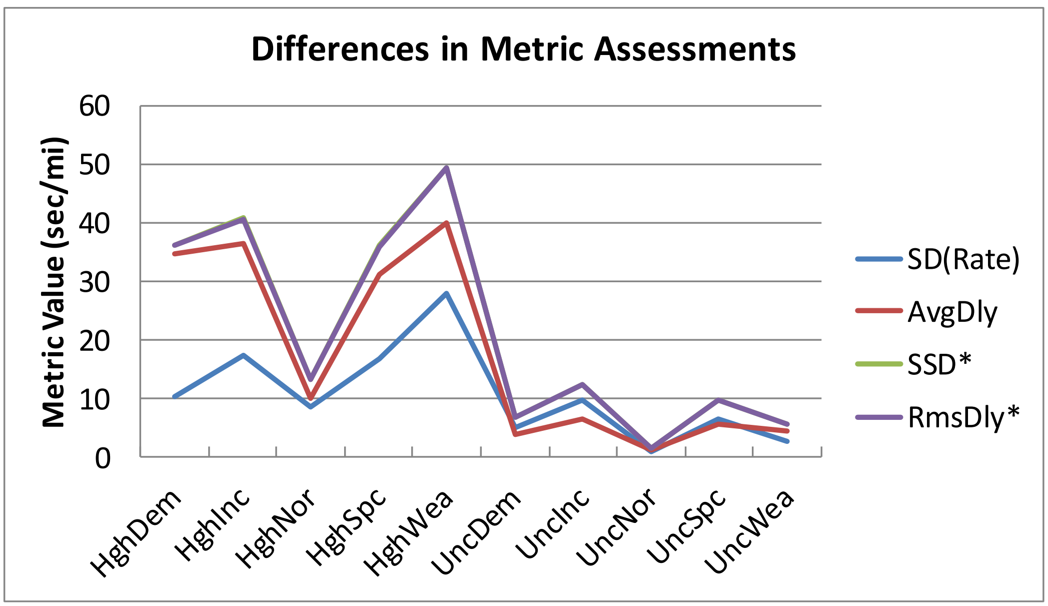

Figure 13. Differences in the variability (unreliability) assessment provided by three metrics for 10 regimes on I-5 in San Diego for 2011. (* = 5th percentile travel rate used for SSD = 50.4 sec/mi.)

A useful display idea can be borrowed from the risk assessment. It plots the RMS delay $\tilde{\delta}_r$ values against the frequency of occurrence. This display is shown in Figure 14.

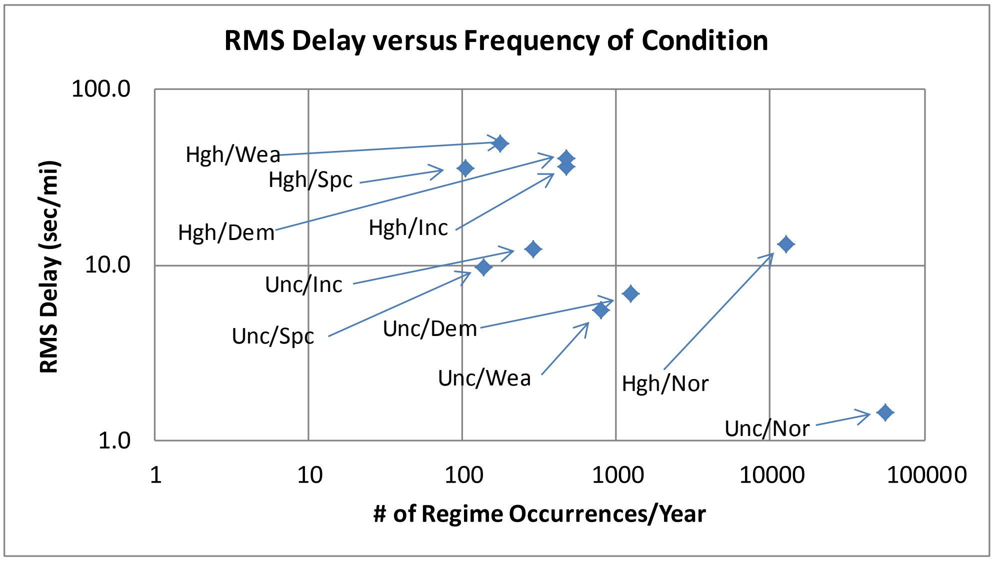

Figure 14. Plot showing the RMS delay values for each regime along with the frequency of occurrence of the regime.

The frequency of condition occurrence is plotted on the *x* axis and the RMS delay $\tilde{\delta}_r$ value is plotted on the *y* axis, both in logarithmic scale because of the major differences in the values involved.

In this display, it is easy to see that the uncongested/normal condition is not a reliability problem. While that condition occurs frequently, its reliability is the highest among all the regimes. The display also shows that there are several conditions having high values of the $\tilde{\delta}_r$ in combination with high frequencies of occurrence. One of these is high congestion/weather. It was noted earlier as possibly being important when the $\tilde{\delta}_r$ values alone were being compared. Not only does this condition have a large $\tilde{\delta}_r$ but it also occurs frequently. Two other conditions worthy of note are high congestion/extra demand and uncongested/weather. They both occur frequently and have high $\tilde{\delta}_r$ values. Not to be overlooked is the high congestion/normal condition which occurs very frequently and also has a high RMS delay. A case could be made that these are the operating conditions on which to focus reliability improvement initiatives.

Pie charts are a possible way to display the reliability metric that is based on the $\tilde{\delta}_r$ values multiplied by the #Obs in Table 5, as shown in the "Severity" column. This calculation is intended to give a sense of the relative importance of the various regimes. It is akin to a vehicle-miles or vehicle-hours measure. For example, the high congestion/normal condition occurs frequently, and it has a somewhat unreliable performance. Perhaps it is the most important. Were this the case, it would be followed by uncongested/normal and then high congestion/incidents.

The pie chart created by this assessment is shown in Figure 15.

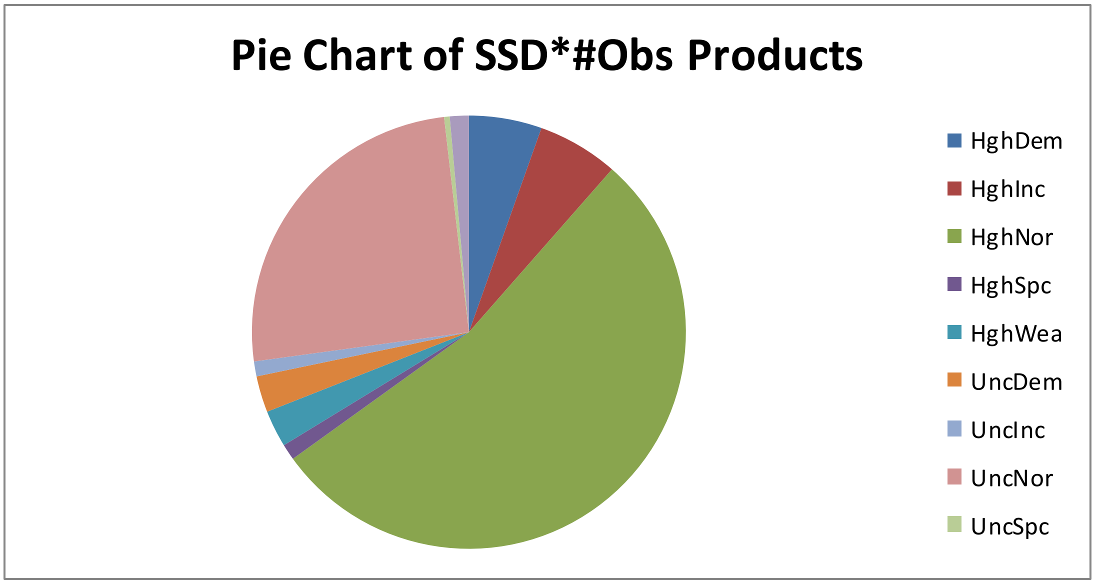

Figure 15. Pie chart showing the result from multiplying the $\tilde{\delta}_r$ values for specific regimes by the frequency with which those regimes occur.

The display, however, can be problematic compared with Figure 10, because the differences in unreliability are not obvious, since they have been multiplied by the frequency of occurrence. (It is not important whether the $\tilde{\delta}_r$ values were used or one of the other variation-related metrics. The pie chart result would effectively be the same. Just the relative proportions would change.)

Displays for a Specific Time Period

The displays presented so far have been based on examining the performance of a system across its "duty cycle": in this case, an entire year.

Often, though, the focus is on the facility's performance during a specific time period, such as the peak period. Agencies sometimes aim to have the highway network provide acceptable travel times during this time on all but one day per month (19 days out of the 20 workdays per month), which leads to an emphasis on metrics like the 95th percentile travel time (19 out of 20 observations).

To illustrate the displays presented above in the context of a peak period, consider the performance of the I-5 route between 15:00 and 19:00, effectively the hours under which I-5 is under heavy load (high congestion). In this case, there are 48 5-minute observations on each of the 250 days, resulting in 12,000 5-minute observations.

The first display, presented in Table 6, shows a breakdown of the 5-minute time periods based on operating regimes. It is easy to see that high/congestion/normal is the most prevalent regime and that it has the lowest RMS delay value. In this case, the RMS delay assessments are based on a 5th percentile value of 51.5 sec/mi. It is also easy to see that the regime with the highest RMS delay is high congestion/weather, and that its reliability is substantially worse than that of the other regimes. It is important to note, though, that this condition does not occur frequently. It arose in only 148 of the 12,000 5-minute time periods. The two abnormal conditions that arose four times as often were high congestion/demand and high congestion/incidents, 458 and 446 5-minute time periods respectively, and that, as a result, they are more substantial in their severity indicators than the weather regime.

Table 6. Reliability Assessment by Regime on I-5 between 3:00–7:00 p.m. in San Diego in 2011

0	1	2	3	4	5	6	7	8	9	10	11
Label	CongCond	NRecCond	nObs	AvgRte	SD(Rte)	AvgInc	RmsDly*	SSD*	SemiVar*	Severity	RelSev
HghNor	High	Normal	10855	61.6	8.8	10.1	13.36	13.74	188.75	145065	76.1
HghDem	High	Demand	458	85.9	9.4	34.4	35.65	35.65	1271.01	16328	8.6
HghInc	High	Incidents	447	88.0	17.1	36.4	40.49	40.53	1642.75	18097	9.5
HghSpc	High	Special Events	95	83.1	16.7	31.5	36.25	36.44	1328.21	3444	1.8
HghWea	High	Weather	149	95.2	27.8	43.4	52.12	52.30	2735.15	7766	4.1
	Total		12004	n/a	n/a	n/a	n/a	n/a	n/a	190701	100.0
		* Note: 5-th percentile travel rate used for SSD =				51.5		sec/mi			

One way to display these data is presented in Figure 16. In it, the RMS delay values for each regime are plotted against the frequency with which the regimes arise during the 3:00–7:00 p.m. peak. As can be seen, the normal condition occurs most often, but its SSD value is the lowest. Three regimes with substantial RMS delay values that occur more frequently are weather, incidents, and high demand. This can serve as the basis for (defense of) mitigating strategies that might be undertaken to improve reliability.

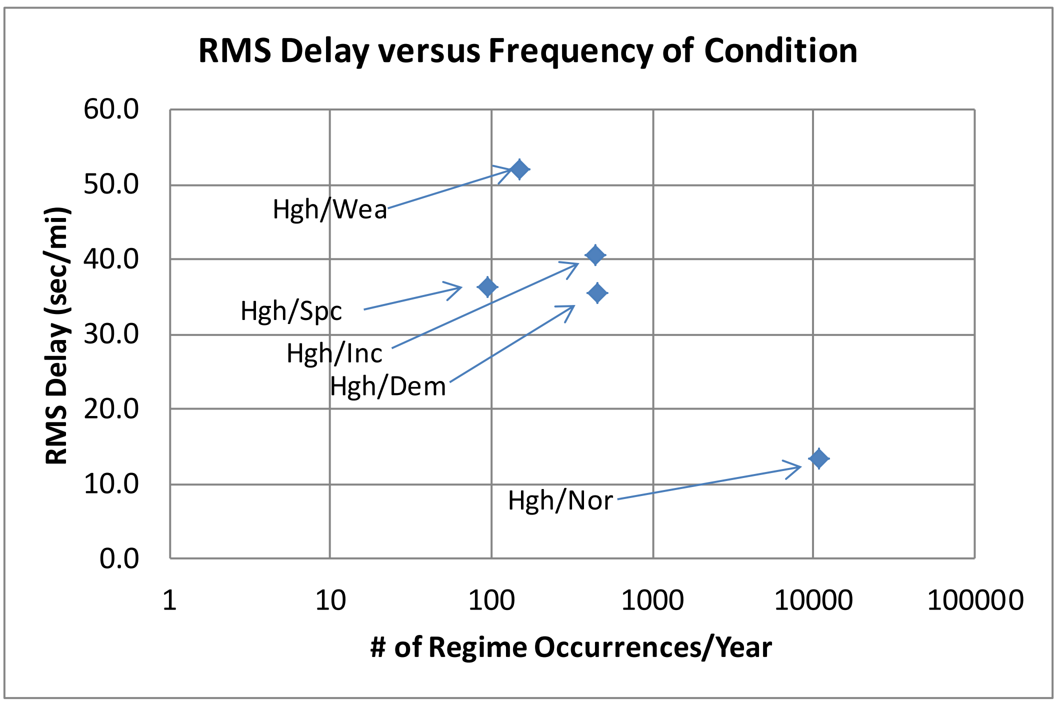

Figure 16. Plot showing the RMS delay values for each regime along with the frequency of occurrence of the regime.

Figure 17 plots this same information in the form of a pie chart. As was indicated earlier, it is important to annotate the chart with the reliability metrics. Part (a) does this for all of the regimes including normal operation. Part (b) does it for only the nonrecurring congestion conditions. The normal value has been zeroed out.

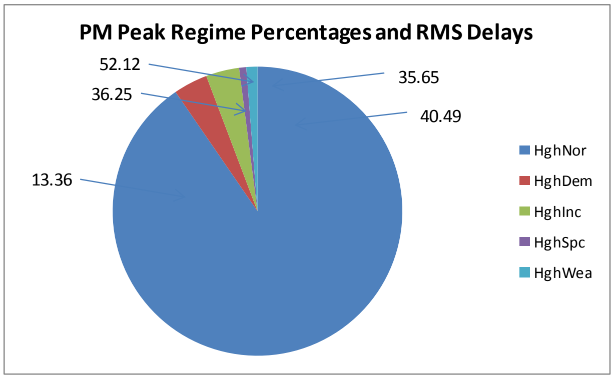

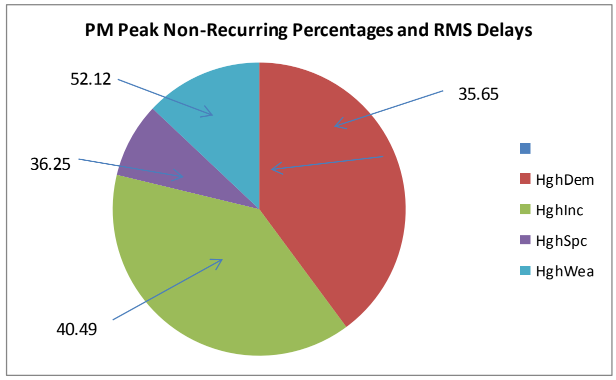

Figure 17. Pie chart breakdowns of the p.m. peak operating regimes and reliability assessments for weekdays on I-5 in San Diego in 2011.

Figure 18 displays the PMFs for the various regimes that are operative during the p.m. peak. As can be seen, the normal regime has the most low value travel rates. Special events and extra demand regimes have greater percentages of higher travel rates, incident regime conditions have even high travel rates, and weather has the highest values. But there is a lot of overlap among the PMFs so the contribution of the individual regimes is hard to see.

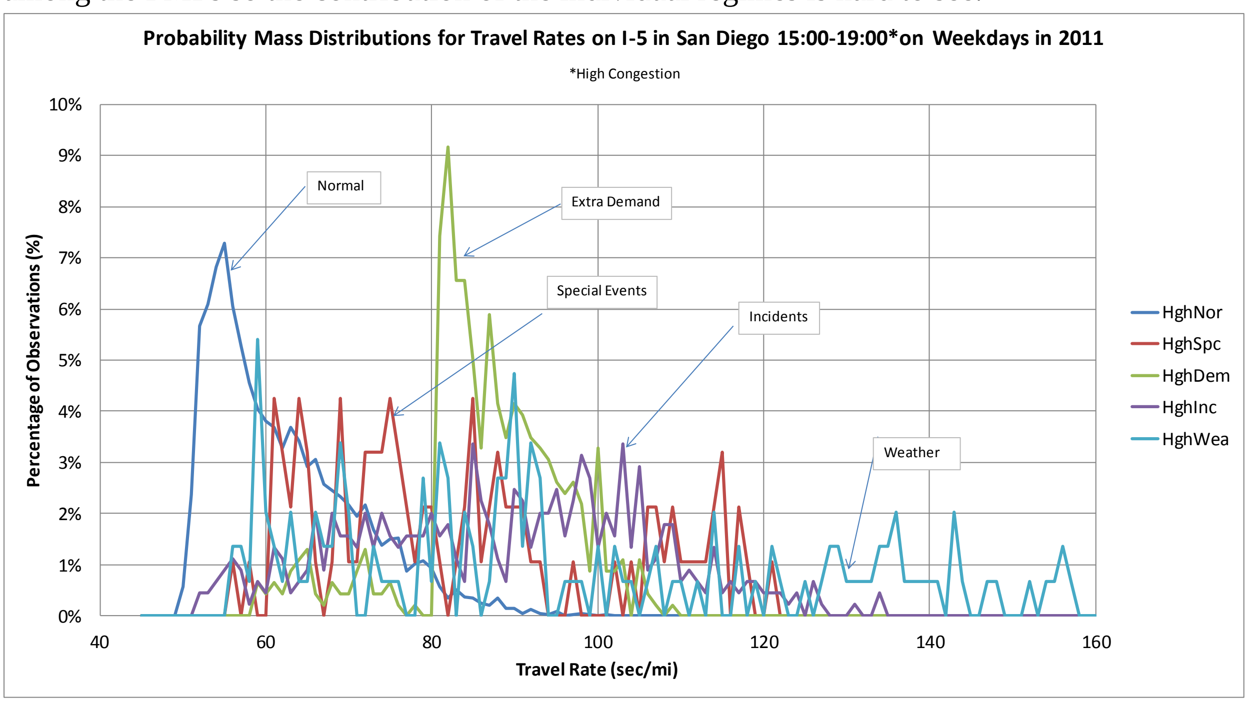

Figure 18. PMFs for travel rates by regime for 3:00–7:00 p.m. on I-5 in San Diego in 2011

Figure 19 displays the same information as shown in Figure 18, only it uses a stacked PMF.

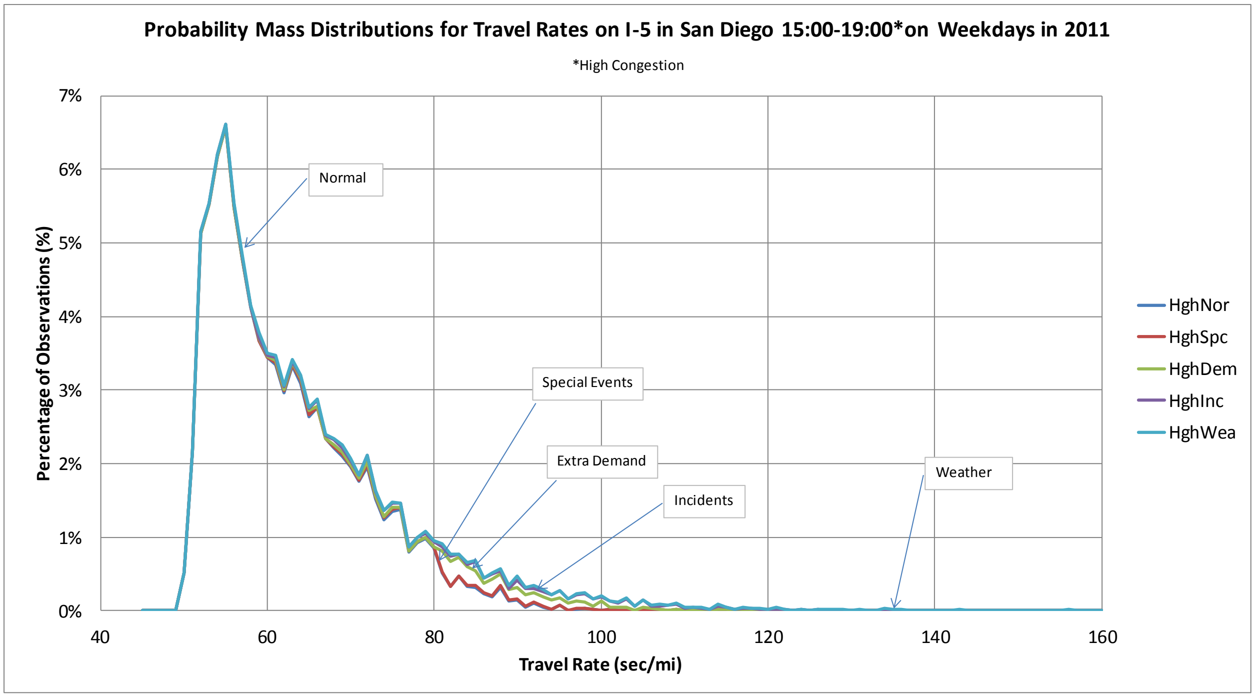

Figure 19. Stacked PMF by regime for 3:00–7:00 p.m. on I-5 in San Diego in 2011.

In this display, the relative contribution of the various regimes to the overall PMF can be seen. It is easy to notice that the normal regime is the most common and contributes most to the overall PMF. It dominates the others. Special events add a little, but very little to the overall distribution. Extra demand adds significantly to the total PMF for travel rates between about 80 and 100 sec/mi. There is a significant difference in the cumulative PMF for normal and special events compared with normal, special events, and extra demand. Incident regimes add more to the overall PMF within this same range of travel rates, and then weather makes the significant contributions for travel rates at or above about 110 sec/mi. This is consistent with Figure 16. The CDFs for these operating regimes tell the same story, only perhaps in a clearer way, as shown in Figure 20.

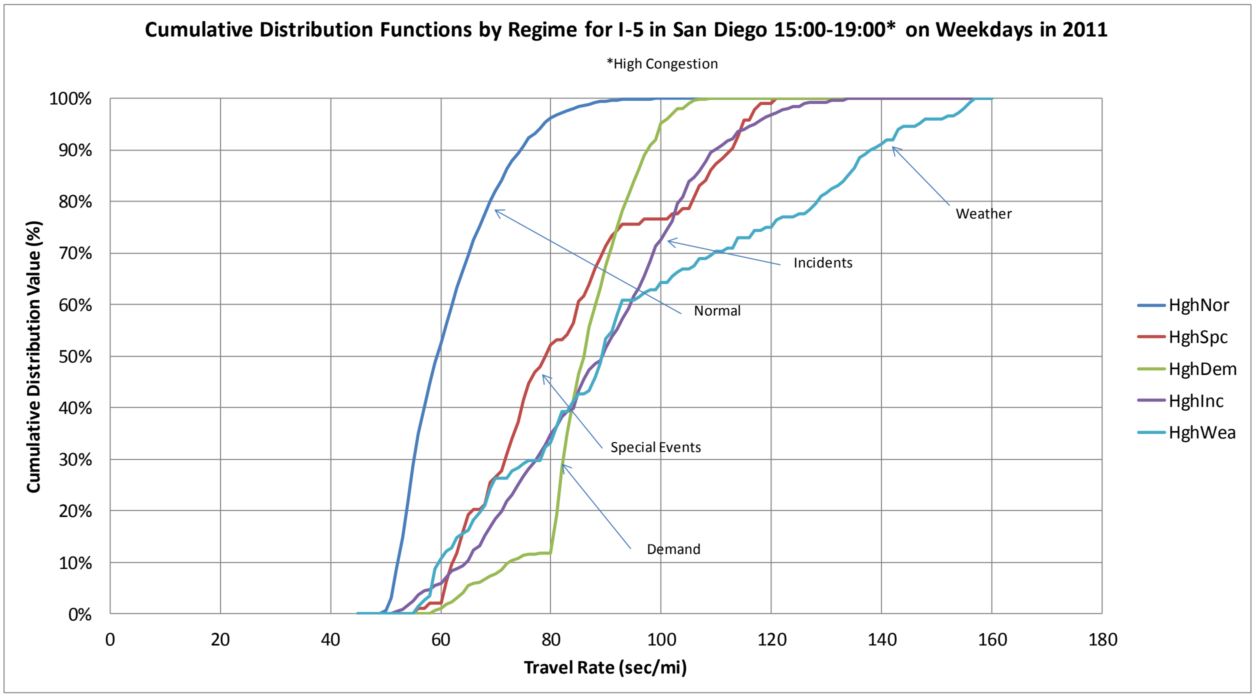

Figure 20. CDFs for travel rates by regime for 3:00–7:00 p.m. on I-5 in San Diego in 2011.

It is easy to see that the normal condition has the best reliability performance. Weather has the worst. The other three regimes—extra demand, special events, and incidents—are in between.

Some agencies use reference travel speeds lower than the free-flow speed. For example, an agency might decide that during the peak hours, speeds above 45 mph are deemed acceptable. This would mean that travel rates less than 80 sec/mi would be acceptable. In this case, the values in Table 4 would change, because a new reference rate was being employed. Now the assessment would be as portrayed in Table 7. The high/normal condition has an RMS delay almost equal to zero, while the RMS delays are still large. The severity values are also very different, but, in spite of the significant change in the reference rate from about 50 sec/mi to 80 sec/mi, the high frequency of occurrence for the normal condition produces a severity metric, which is still very large. So the severity index is still not providing particularly insightful guidance about what actions to take.

Table 7. Alternate Reliability Assessment on I-5 between 3:00-7:00 p.m. in San Diego in 2011

0	1	2	3	4	5	6	7	8	9	10	11
Label	CongCond	NRecCond	nObs	AvgRte	SD(Rte)	AvgInc	RmsDly*	SSD*	SemiVar*	Severity	RelSev
HghNor	High	Normal	10855	61.6	8.8	0.2	1.31	6.75	45.60	14211	43.4
HghDem	High	Demand	458	85.9	9.4	7.5	10.02	10.67	113.76	4588	14.0
HghInc	High	Incidents	447	88.0	17.1	12.0	17.51	21.70	470.81	7826	23.9
HghSpc	High	Special Events	95	83.1	16.7	8.9	15.56	22.61	511.38	1479	4.5
HghWea	High	Weather	149	95.2	27.8	19.9	31.06	38.10	1451.54	4627	14.1
	Total		12004	n/a	n/a	n/a	n/a	n/a	n/a	32731	100.0
		* Note: 5-th percentile travel rate used for SSD =				80.0		sec/mi			

Figure 21 presents the revised RMS delay values from Table 5 for each regime plotted against the frequency with which the regimes arise during the 3:00–7:00 p.m. peak.

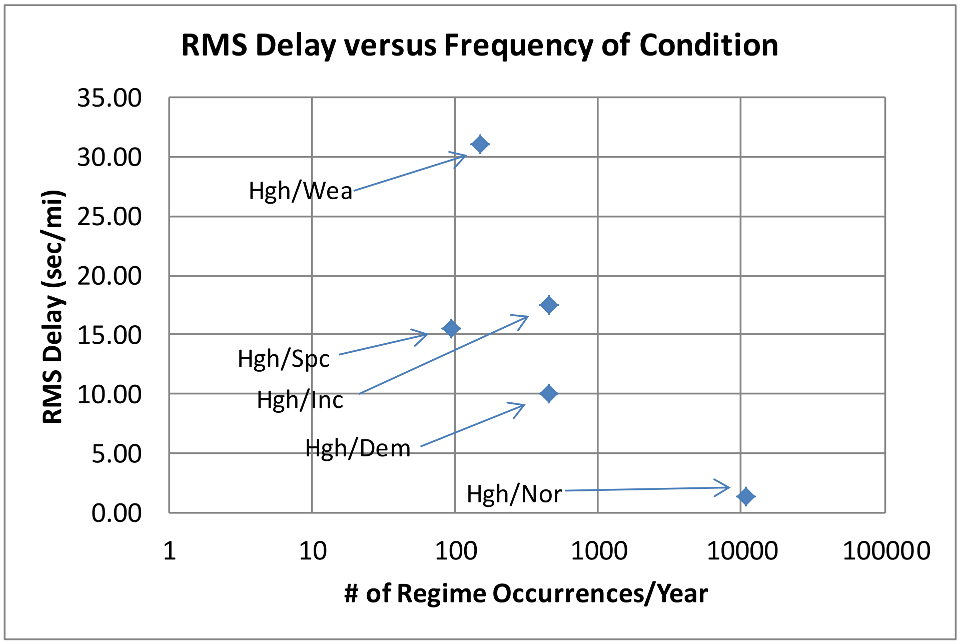

Figure 21. Revised plot showing the RMS delay values for each regime along with the frequency of occurrence of the regime for a condition where the reference travel rate is 80 sec/mi (45 mph).

As can be seen, the normal condition occurs most often, but its RMS delay value is the lowest, nearly zero. The three regimes with substantial RMS delay values that occur frequently are weather, incidents, and high demand. This can serve as the basis for (defense of) mitigating strategies that might be undertaken to improve reliability.

Displays Across Time

As illustrated previously by Figure 6, reliability performance varies by time of day. An assessment of how it varies is important. Table 8 presents such an assessment for the I-5 route in

San Diego. The time periods are: Early morning (0:00–6:55), a.m. peak (7:00–8:55), midday (9:00–14:55), p.m. peak (15:00–18:55), and evening (19:00–11:55). Other breakdowns are possible.

Table 8. Time-Period-Based Assessment on I-5 between 3:00–7:00 p.m. in San Diego in 2011

	1	2	3	4	5	6	7	8	9	10
Time Period	CongCond	NRecCond	nObs	AvgRate	SD(Rate)	AvgDly	RmsDly*	SSD*	SemiVar*	Severity
0-Early AM	Uncon	Demand	613	53.2	1.1	2.8	3.07	3.07	9.42	1882
0-Early AM	Uncon	Incidents	61	53.0	0.0	2.6	2.99	3.01	9.08	182
0-Early AM	Uncon	Normal	20079	51.3	0.6	1.0	1.19	1.23	1.51	23848
0-Early AM	Uncon	Weather	250	53.9	0.0	3.6	4.14	4.15	17.19	1035
1-AM Peak	Uncon	Demand	159	58.3	10.4	8.0	13.78	13.83	191.16	2191
1-AM Peak	Uncon	Incidents	36	52.9	0.0	2.3	2.53	2.56	6.57	91
1-AM Peak	Uncon	Normal	5760	51.5	0.6	1.1	1.47	1.49	2.23	8444
1-AM Peak	Uncon	Weather	49	61.8	0.0	11.4	11.80	11.92	142.15	578
2-Midday	High	Demand	17	59.3	0.0	8.2	9.43	9.72	94.51	160
2-Midday	High	Incidents	26	64.6	0.0	13.9	15.33	15.63	244.25	398
2-Midday	High	Normal	2165	53.4	1.2	3.0	3.52	3.53	12.48	7630
2-Midday	High	Special Events	15	66.2	0.0	15.6	18.18	18.82	354.24	273
2-Midday	High	Weather	32	65.1	0.0	14.2	16.35	16.61	275.78	523
2-Midday	Uncon	Demand	187	56.9	5.6	6.4	9.76	9.79	95.79	1825
2-Midday	Uncon	Incidents	93	56.6	0.0	6.2	7.20	7.24	52.43	670
2-Midday	Uncon	Normal	15327	52.0	1.0	1.7	1.98	2.00	4.00	30335
2-Midday	Uncon	Weather	147	58.2	0.0	7.9	8.46	8.49	72.01	1243
3-PM Peak	High	Demand	457	85.9	9.0	35.6	36.80	36.84	1357.31	16818
3-PM Peak	High	Incidents	442	88.3	16.9	37.9	41.71	41.76	1743.57	18435
3-PM Peak	High	Normal	10620	61.8	8.8	11.4	14.41	14.47	209.45	153064
3-PM Peak	High	Special Events	91	84.0	16.5	33.5	37.95	38.16	1456.40	3454
3-PM Peak	High	Weather	145	96.2	27.5	45.6	53.80	53.99	2914.79	7801
3-PM Peak	Uncon	Demand	3	75.5	0.0	9.9	12.80	15.68	245.93	38
3-PM Peak	Uncon	Incidents	6	64.7	0.0	10.1	19.47	21.33	455.12	117
3-PM Peak	Uncon	Normal	236	52.2	0.0	1.9	2.71	2.94	8.63	640
3-PM Peak	Uncon	Special Events	5	61.2	0.0	10.5	13.14	14.69	215.86	66
3-PM Peak	Uncon	Weather	5	59.6	0.0	7.1	8.27	9.24	85.42	41
4-Evening	Uncon	Demand	292	53.0	0.0	2.6	3.73	3.73	13.94	1088
4-Evening	Uncon	Incidents	94	60.9	15.3	10.5	19.37	19.47	379.17	1821
4-Evening	Uncon	Normal	14136	51.1	0.4	0.7	0.94	0.98	0.96	13218
4-Evening	Uncon	Special Events	132	55.7	6.4	5.4	9.43	9.51	90.38	1245
4-Evening	Uncon	Weather	351	53.0	0.0	2.6	2.88	2.89	8.33	1012

From the display, it is easy from the RMS details to see that the worst reliability is associated with weather events during the p.m. peak. The next worst is incidents during the p.m. peak, and then special events during the p.m. peak. This information, combined with the frequency of occurrence, can easily be used to identify and prioritize mitigation strategies. An interesting display option takes this same information and develops PMFs for short time slices across the day. Depicted in Figure 22 is a display of average travel time PMFs for two routes in the San Francisco Bay Area.

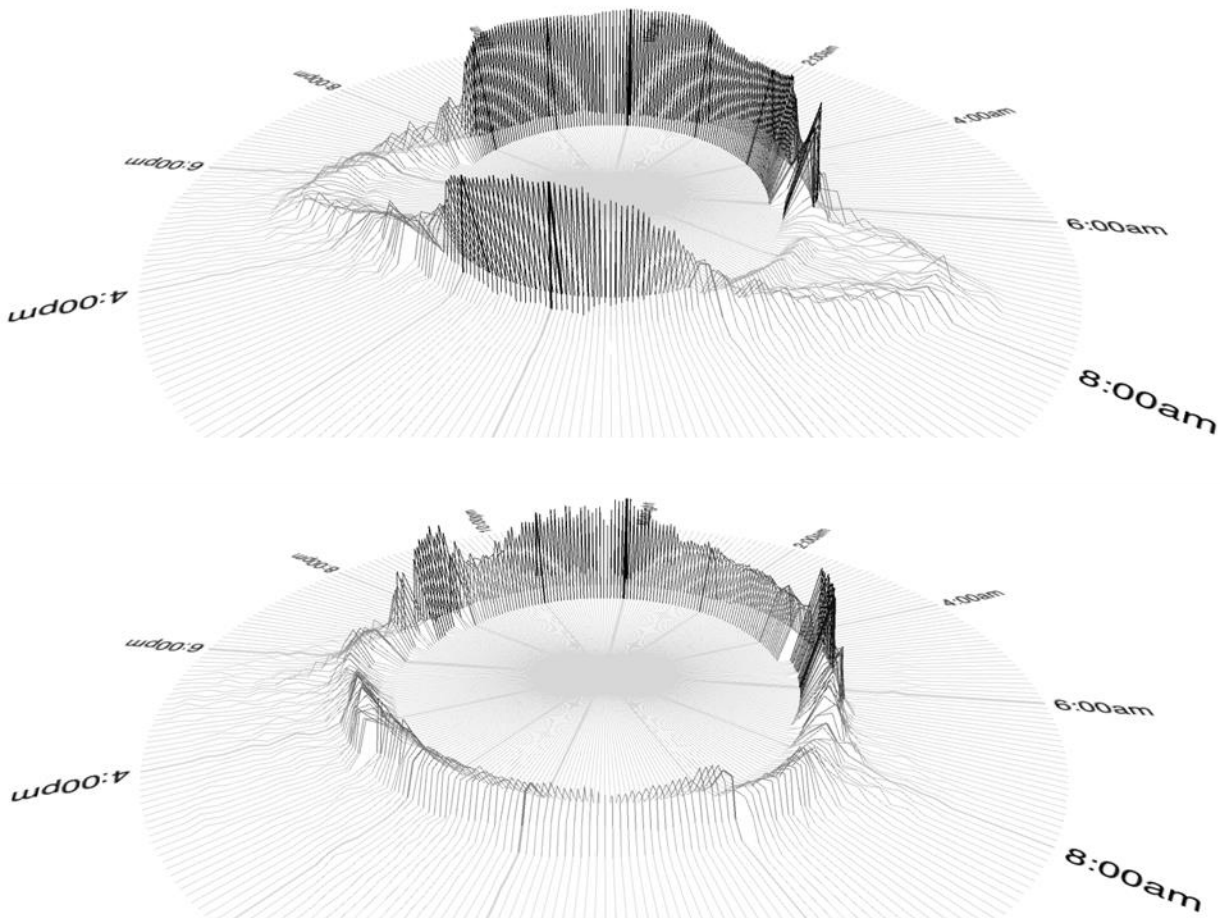

Figure 22. Display of travel time PMFs by time of day.

The PMFs are arrayed in chronological order in a radial fashion. Times of day are identified (with time progressing clockwise) so that it is possible to see how the PMFs vary by time of day. It is easy to see that the travel times during the off-peak time periods are far more reliable than during the peaks. During the off-peak time periods, all of the travel times are concentrated around a minimum value while, during the peak time periods, the distributions are widely distributed with very large travel times sometimes occurring. It is also easy to see that the performance of the first route is much worse than the second. That is to say that for the first route, the travel times during the peak hours increase substantially more, and there is more variation in the values.

A variant on this plot is shown in Figure 23. Displayed are CDFs for individual vehicle travel times during specific half-hour time periods during the winter of 2012. From this display, it is easy to see that the distribution of travel times deteriorates as time progresses through the peak until the 17:00–17:30 half hour is reached. Then, the travel times begin to decrease. A display like this can be very useful, especially if it is animated, to see how the reliability varies by time of day, and to see how mitigation actions improve that performance.

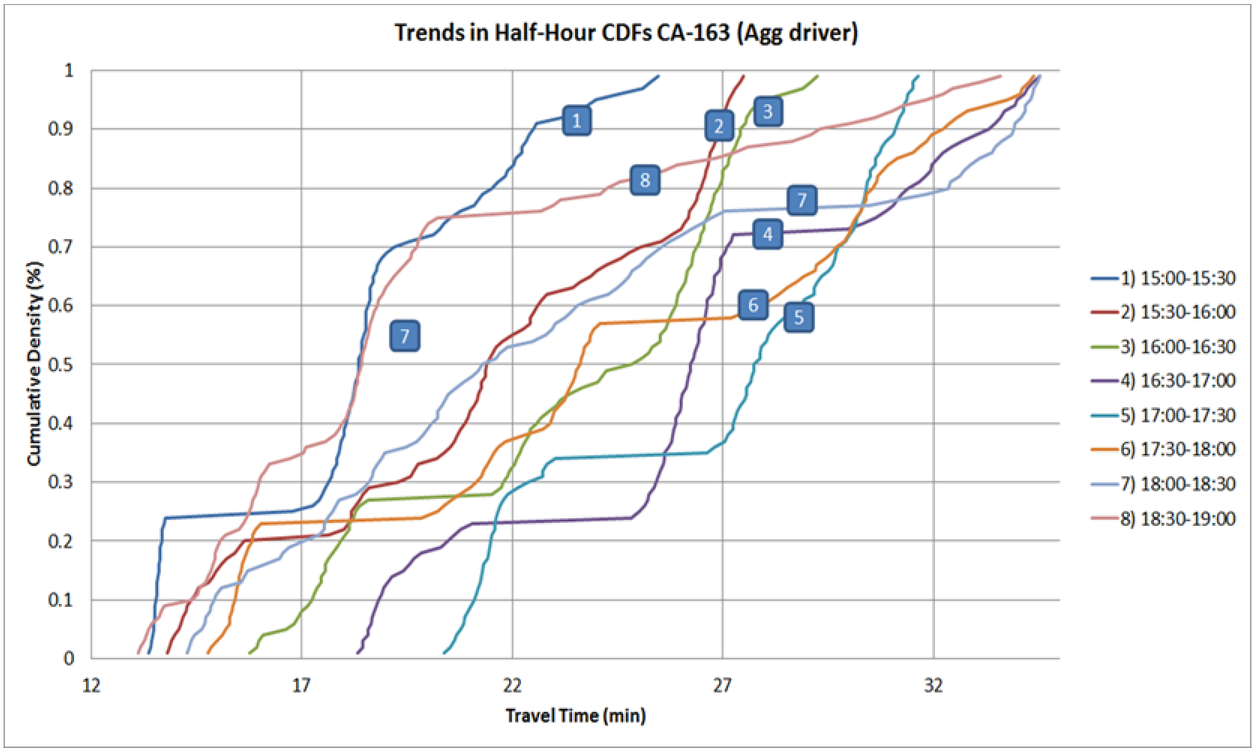

Figure 23. Display of travel time CDFs during the p.m. peak on I-5 in Sacramento during the winter of 2011.

A third variant on this set of display options is a time-based display of the way in which the percentiles of the travel times vary by time of day. This is shown in Figure 24. Each vertical set of symbols shows the locus of specific percentiles of the vehicle-to-vehicle travel time distribution at a specific point in time. It is easy to see that at about 11:00 a.m. on this particular day, there was an incident. All of the travel time percentiles increased. Some percentiles increased more than others. Operating conditions were back to normal by about 11:45. Then, at about 16:00, the p.m. peak commenced. The percentiles began to increase, especially the lower percentiles (the standard deviation actually decreased) and then all of the percentiles increased as the p.m. peak progressed. The highest percentile values occurred at about 18:00, and then the travel times began to decrease. By about 18:30, the percentiles were back to the values that were observed before the peak commenced.

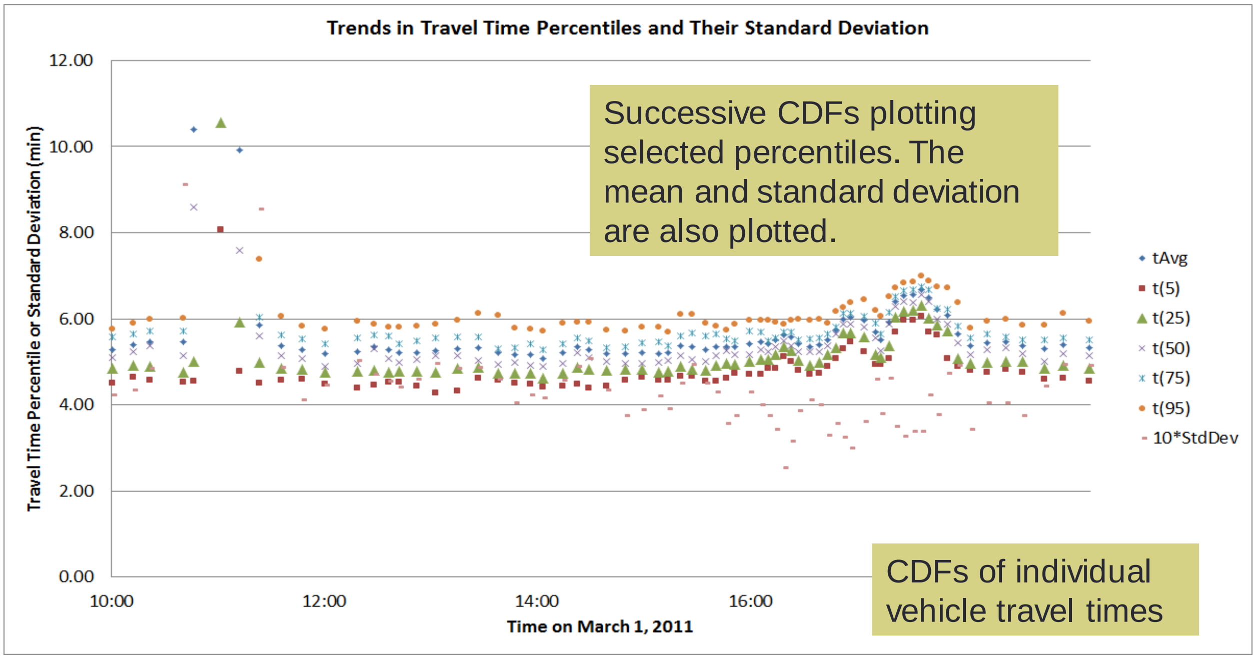

Figure 24. Display of travel time CDFs during the p.m. peak on I-5 in Sacramento on March 1, 2011.

Displays for Routes and Networks

In some instances, a reliability assessment focuses on routes between specific origin-destination (O-D) pairs or interconnected segments in a network. In this case, the spatial relationship among the segments is important.

A number of other display options are possible. These displays are typically map-based and present a network-level image of reliability.

From a path choice perspective, reliability is one of a number of metrics involved in determining which route to select. Distance is one, cost is another, the percentage use of freeways (or arterials) might be a third, and the minimum possible travel time might be a fourth. The travelers want to make a tradeoff analysis among these metrics in determining which path to select.

Two illustrations of this thought are shown in Figure 25. In the case of the illustration on the left, three routes are being suggested, and the travel times and distances for each are displayed. Not displayed are other attributes that the traveler might also apply in determining which route to select, such as reliability and tolls. In the illustration on the right, again three possible routes are being displayed, in this case between Fresno and Los Angeles. While the attribute values for the second and third routes are not explicitly displayed, it is easy to see that there would likely be differences in both travel time and distance and that the suggested route might be best. Again, the traveler might be aware of other differences like reliability and the types of facilities employed, which might influence the decision about which route to select.

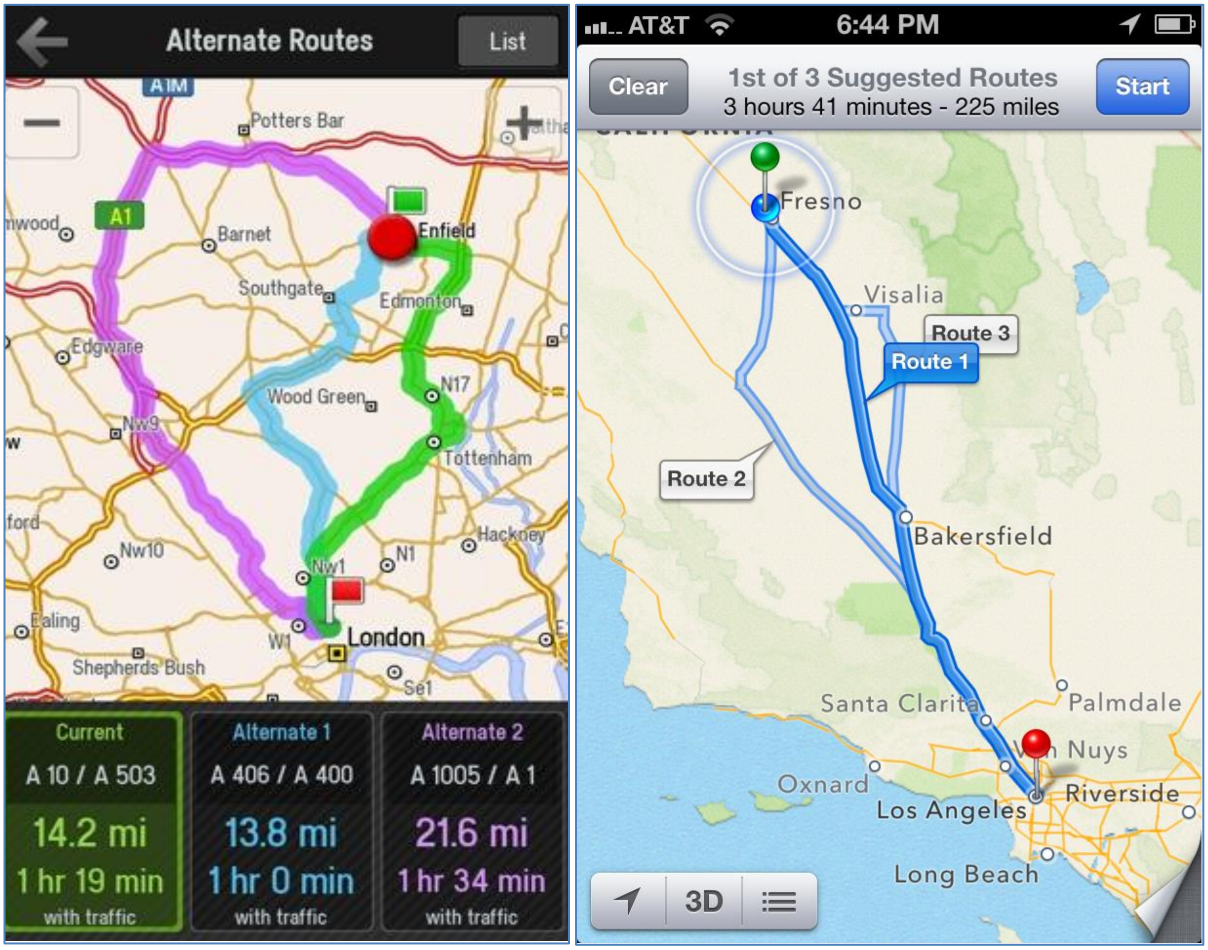

Figure 25. Display of routing options.

Reliability is an additional metric whose characteristics can be displayed in this manner. In the case of Figure 26, Harvey Balls are being used to present information about the reliability of the various segments. Solid white implies high reliability, and solid black implies poor reliability.

If a traveler were to examine such a map in making route choice, determining which route choice based on reliability might be easy. The path A-B-D-F-G would have the best overall reliability and A-C-E-F-G the worst. The metric employed in shading the Harvey Balls could be the RMS delay used earlier or some other reliability-based metric.

Not only can travelers use such a display for choosing among paths but network managers can also use such displays to prepare route guidance information for variable message signs, highway advisory radio, and route guidance apps. Such a display also helps them determine where the problematic segments are so they can determine what mitigating actions to take. In this instance, it appears that the most important segments on which to focus are CB, CE, and CF.

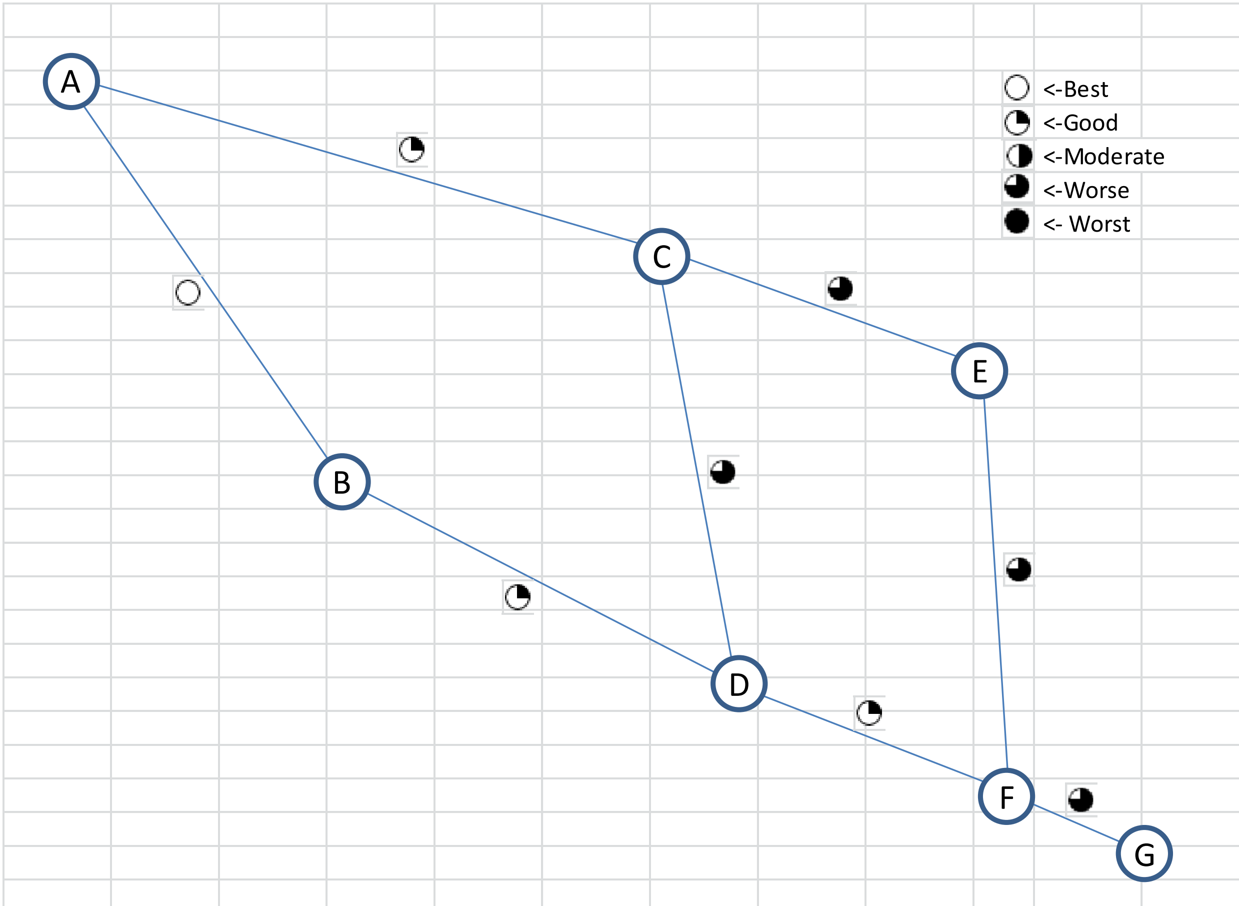

Figure 26. Using Harvey Balls to display reliability.

Another option for displaying the reliability information presents both the mean travel time and the variability (variance) in the travel time. As shown in Figure 27, in this instance two colors are used to display the information for each segment. The wider dash is used to display the mean, and the narrower one is used to display the standard deviation. Green implies a low value, red implies a high value, and yellow is in between. It is immediately apparent that segment AB has the best performance. It has a low average travel time and a low standard deviation. Segments CD and CE are the worst, having high average travel times and high standard deviations.

Since the mean and standard deviation are both being displayed, it is possible to see additional information about segments like AC and EF. In the first instance, the average travel time is low while the standard deviation is high. This segment is likely to be viewed as being unreliable. In contrast, segment EF has a high average travel time but its standard deviation is low. So its reliability might be viewed as being good in spite of the fact that the average travel time is high. The travel times are consistent.

As was the case with the information displayed in Figure 26, path A-B-D-F-G would likely be the best from a reliability standpoint. Path A-C-D-F-G might be the worst. It has the worst combination of standard deviation values. Path A-C-E-F-G might have a longer average travel time, but its standard deviation would likely be smaller, so it might be deemed more reliable than A-C-D-F-G.

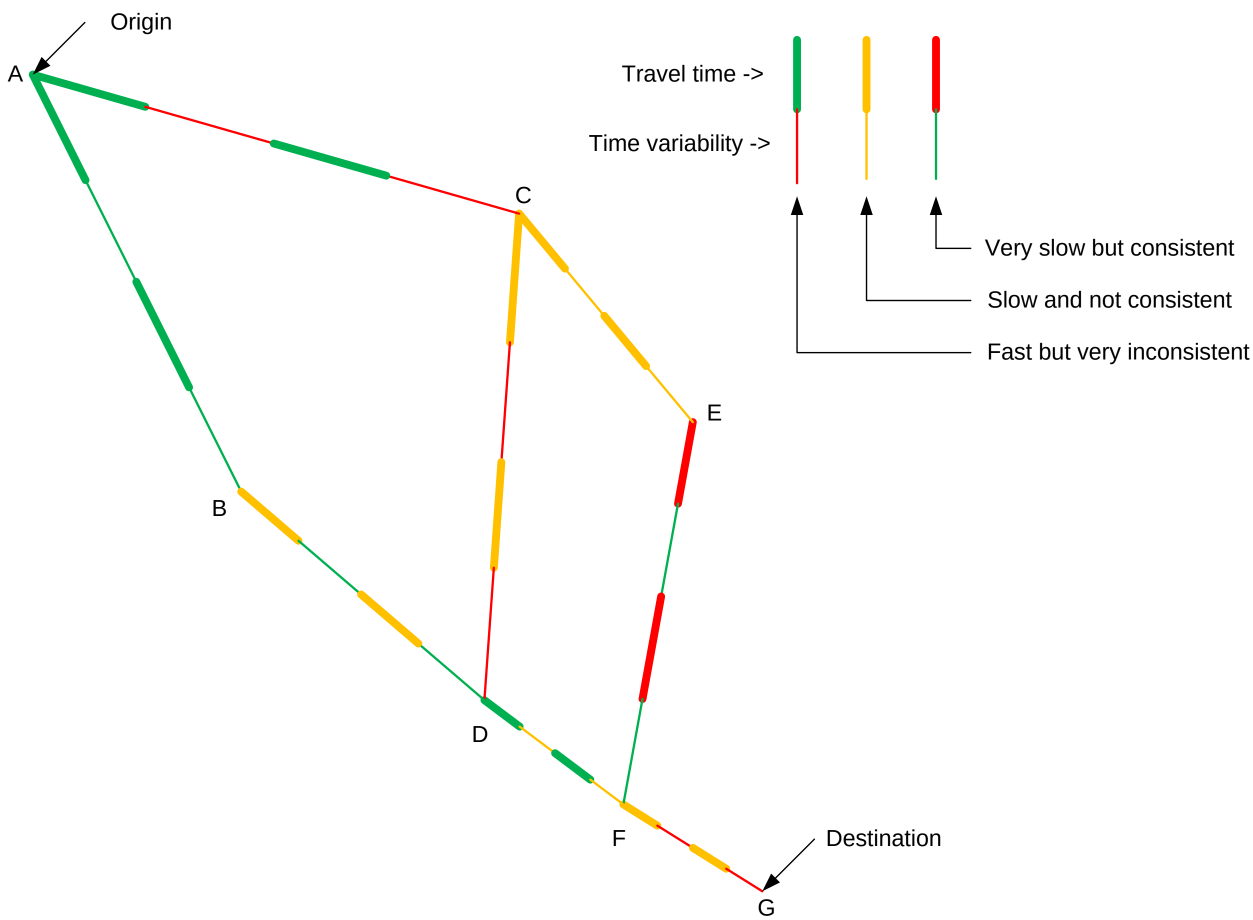

Figure 27. Displaying segment mean travel times and standard deviations.

An alternate presentation of the exactly the same information is displayed in Figure 28. In this instance, Harvey Balls are being used to present the mean travel times and standard deviations instead of colors. As was the case before, a clear ball implies a low value, and a solid ball implies a high value. In this instance, since each ball can be partially shaded, finer gradations in the assessment can be displayed. For the graphic presented, four levels of differentiation are possible. Of course, with more sophisticated Harvey Balls, an infinite degree of variation can be displayed.

As was the case with Figure 27, it is possible to see additional information about segments like AC and EF. It is again apparent that segment AC is likely to be perceived as being unreliable because its standard deviation is high. In contrast, segment EF is likely to be seen as being reliable. It has a low standard deviation. It depends on whether the high travel time is factored into the reliability assessment or not.

Also, as was the case with Figure 27, it is easy to compare and contrast the paths in terms of their mean travel times and travel time variability. Path A-B-D-F-G would likely be the best. Path A-C-D-F-G might be the worst. Path A-C-E-F-G might have a longer average travel time, but its standard deviation would likely be smaller, so it might be deemed more reliable than A-C-D-F-G.

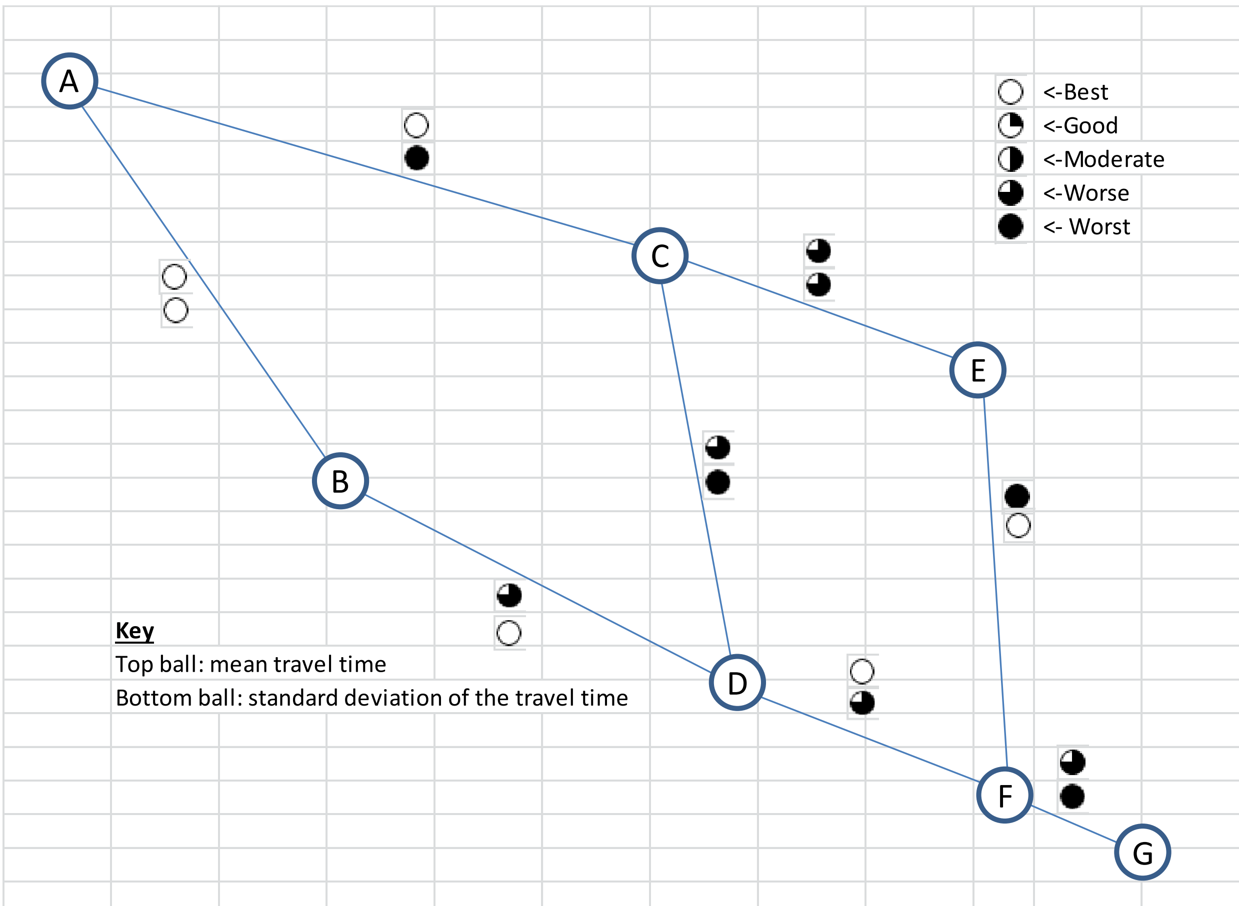

Figure 28. Using Harvey Balls to display segment mean travel times and standard deviations.

Additional Display Options

Other display options have been used by traffic management centers nationwide. Color-coded maps are common, with the colors depicting speeds on individual highway segments, periodically updated. Incidents and construction areas are also almost always shown along with other significant landmarks, like airports.

Maps are often used, supplemented by tables, as illustrated in Figures 29 and 30. This display depicts travel times, speeds, and distances for instrumented highways. In this case, the information includes current travel time, average travel time, distance, and current average speed. The speeds and travel times currently come from point sensors. The level of congestion is also identified with a green, yellow, or red dot, except for the segments that are not instrumented.

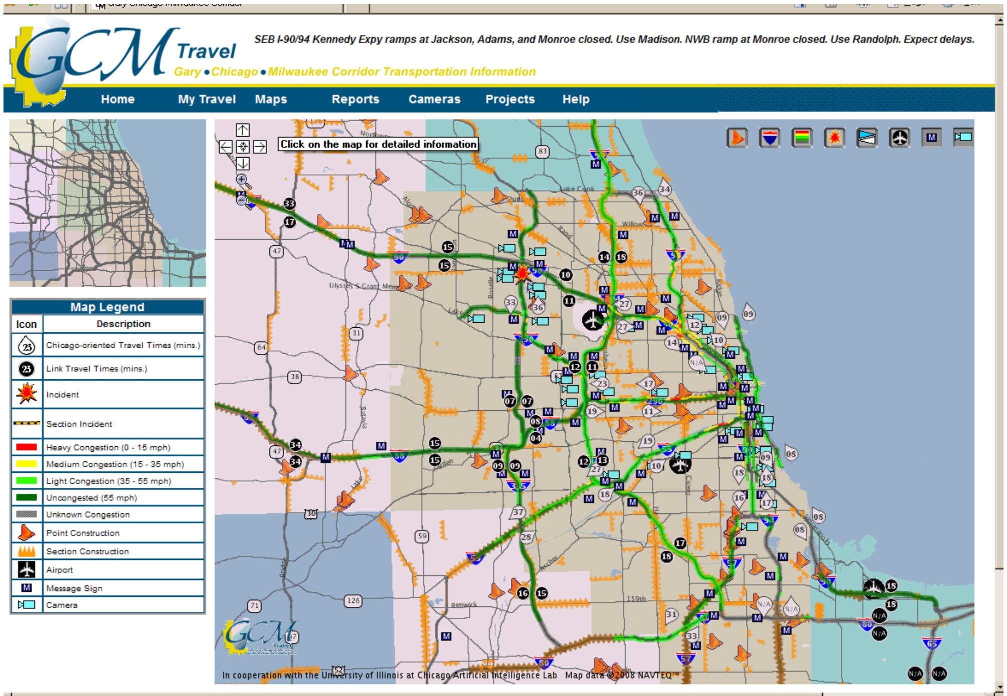

Source: www.travelmidwest.com; accessed 6/22/2009.

Figure 29. Traffic speeds map for the Greater Chicago Metro Area.

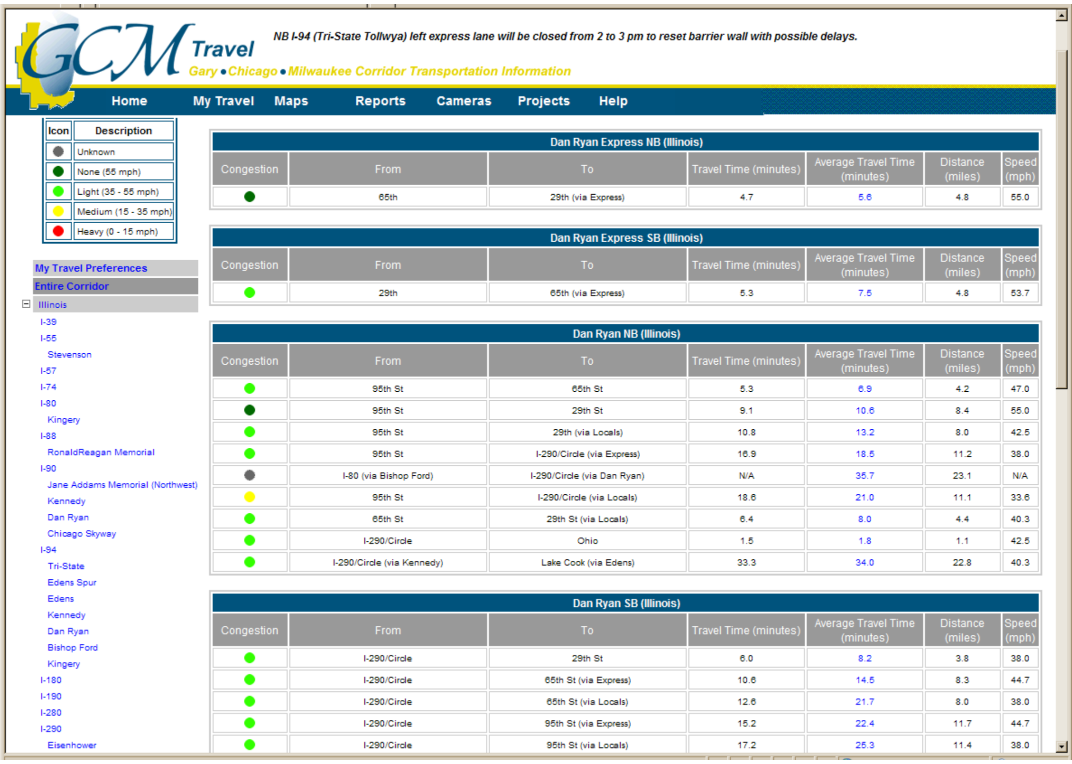

Dan Ryan Express NB (Illinois)

Congestion	From	To	Travel Time (minutes)	Average Travel Time (minutes)	Distance (miles)	Speed (mph)
	65th	29th (via Express)	4.7	5.6	4.8	55.0

Dan Ryan Express SB (Illinois)

Congestion	From	To	Travel Time (minutes)	Average Travel Time (minutes)	Distance (miles)	Speed (mph)
	29th	65th (via Express)	5.3	7.5	4.8	53.7

Dan Ryan NB (Illinois)

Congestion	From	To	Travel Time (minutes)	Average Travel Time (minutes)	Distance (miles)	Speed (mph)
	95th St	65th St	5.3	6.9	4.2	47.0
	95th St	29th St	9.1	10.6	8.4	55.0
	95th St	29th (via Locals)	10.8	13.2	8.0	42.5
	95th St	I-290/Circle (via Express)	16.9	18.5	11.2	38.0
	I-80 (via Bishop Ford)	I-290/Circle (via Dan Ryan)	N/A	35.7	23.1	N/A
	95th St	I-290/Circle (via Locals)	18.6	21.0	11.1	33.6
	65th St	29th St (via Locals)	6.4	8.0	4.4	40.3
	I-290/Circle	Ohio	1.5	1.8	1.1	42.5
	I-290/Circle (via Kennedy)	Lake Cook (via Edens)	33.3	34.0	22.8	40.3

Dan Ryan SB (Illinois)

Congestion	From	To	Travel Time (minutes)	Average Travel Time (minutes)	Distance (miles)	Speed (mph)
	I-290/Circle	29th St	6.0	8.2	3.8	38.0
	I-290/Circle	65th St (via Express)	10.6	14.5	8.3	44.7
	I-290/Circle	65th St (via Locals)	12.6	21.7	8.0	38.0
	I-290/Circle	95th St (via Express)	15.2	22.4	11.7	44.7
	I-290/Circle	95th St (via Locals)	17.2	25.3	11.4	38.0

Source: www.travelmidwest.com; accessed 6/22/2009.

Figure 30. Current congestion and travel times for a freeway segment.

For this Chicago website, drilling down into the average travel time field yields a more detailed picture, and one that is useful in terms of travel time reliability. Figure 31 shows that for this freeway segment and direction, the current travel time is 10.88 minutes, the average is 13.17, the difference is –2.29 minutes, and the average is based on 186 sample days. The time-of-day trend shows high travel times in the a.m. peak that start to rise about 5:00 a.m. and return to nominal night-time, free-flow conditions by about 3:00 p.m. On the day when the website was visited (7/28/2009), unlike most days, there was a major spike in travel time at 2:30 p.m., most likely caused by an incident. The yellow band shows the normal range of travel times (apparently plus or minus one standard deviation as evidenced by the reference to 68%) and the blue lines indicate travel times at free-flow speed (55 mph), medium traffic congestion (35 mph), and heavy congestion (15 mph).

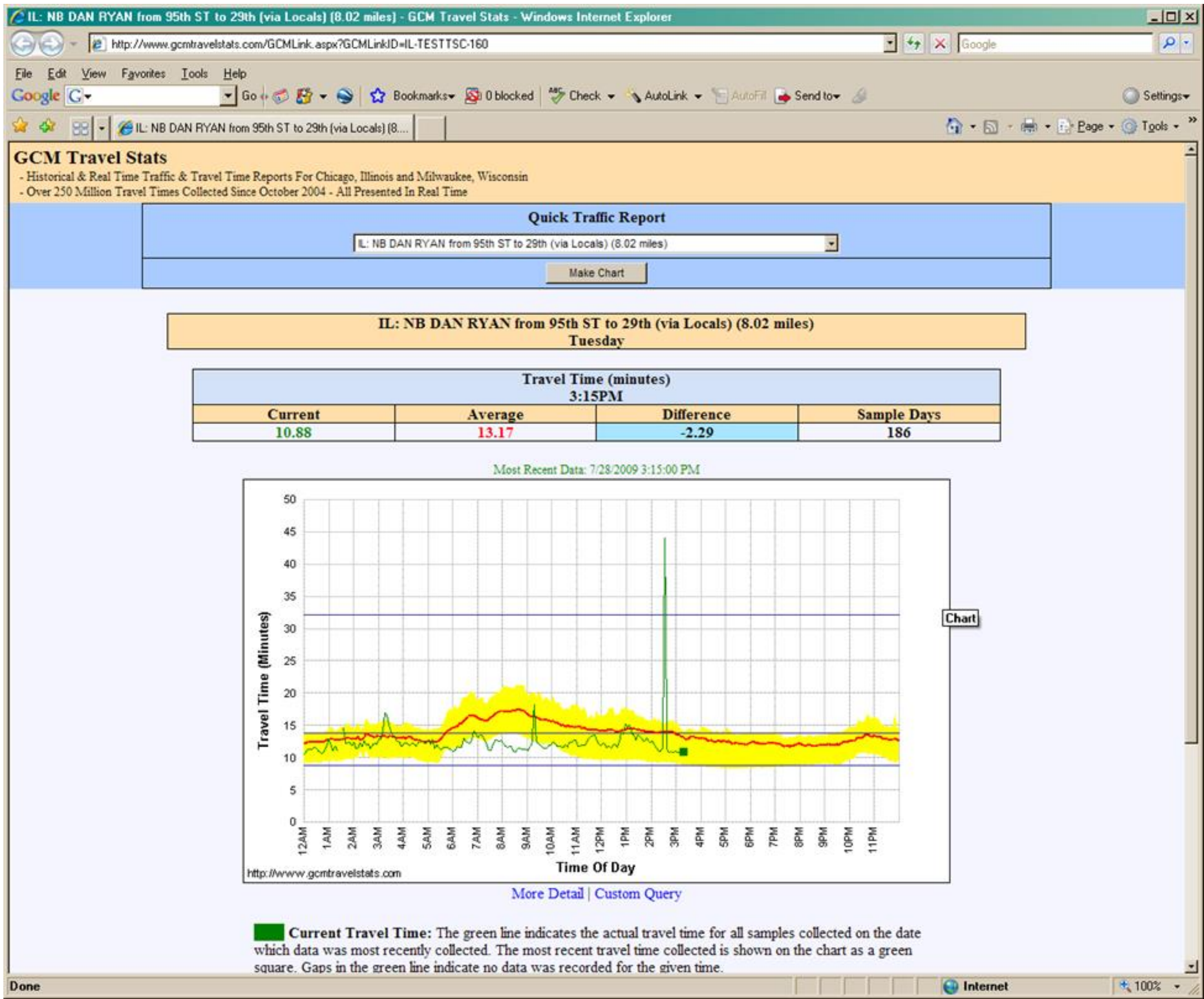

Source: www.travelmidwest.com; accessed 7/28/2009.

Figure 31. Travel time reliability trends for a freeway segment.

A website that directly addresses travel time reliability (really, consistency) is the one used in Seattle. While the color-coded map of traffic conditions looks typical of most sites, as shown in Figure 32, there are lower levels that provide additional detail.

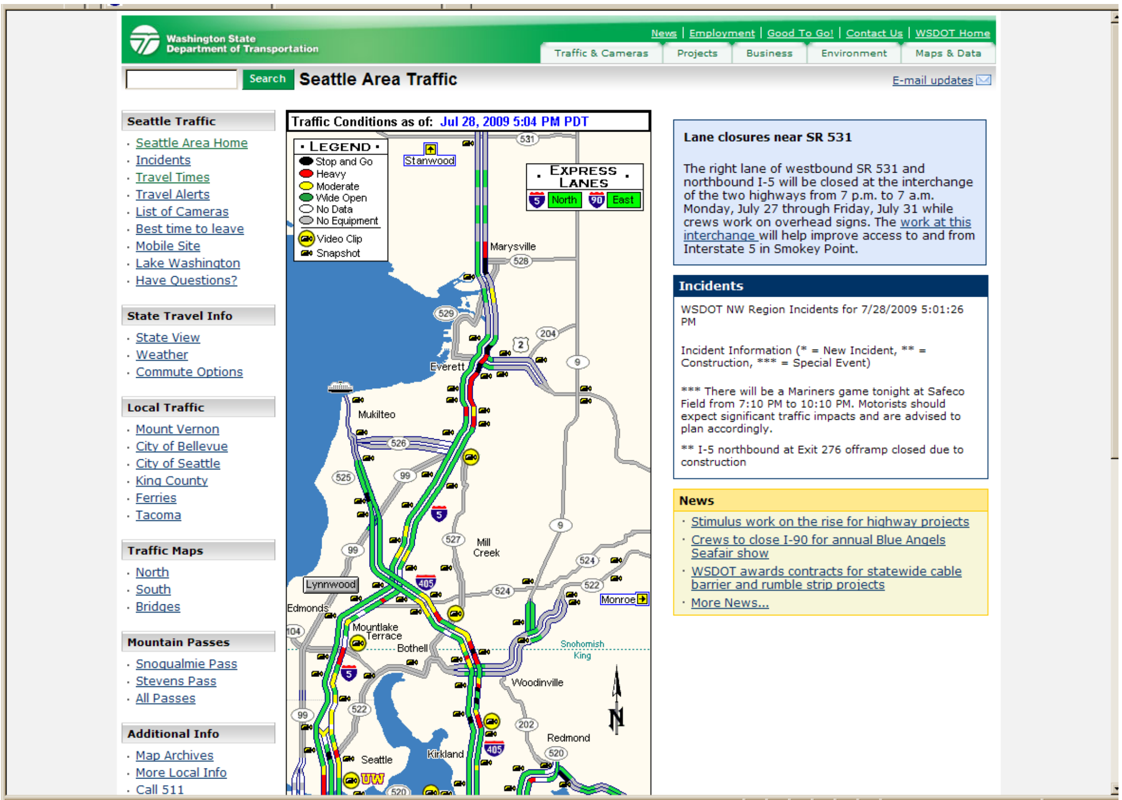

Source: www.wsdot.com/traffic/seattle/default.aspx; accessed 6/22/2009.

Figure 32. Seattle Area traffic conditons map.

Clicking the "Best time to leave" hotlink on the lefthand side leads in two clicks to the tool shown in Figure 33.

Source: www.wsdot.com/traffic/seattle/default.aspx; accessed 6/22/2009.

Figure 33. 95% reliable travel times calculator.

This display allows the traveler to specify an origin and a destination and receive an estimate of the time one needs to allow one to ensure that for 19 out of 20 trips (95% of the time) the destination will be reached on time. In the example window, a trip from Lynnwood to Bellevue is to be completed by 9:00 a.m. The website reports back that the traveler needs to leave Lynnwood at 8:08 a.m. and allow 52 minutes for the trip to ensure that the destination will be reached by 9:00 a.m. However, it should be noted that the resultant text shown in Figure 33 can be confusing or misleading to the average driver. It states in the dialogue box, "Your 95% Reliable Travel Time is 52 minutes. 95% of the time you would need to leave at **8:08 AM** to arrive by 9:00 AM." The WSDOT text may be misinterpreted to mean that if you leave after 8:08 a.m., then 95% of the time you will be late.

Another display option is shown in Figure 34. It depicts directions and driving times for one or more routes, including the current level of delay.

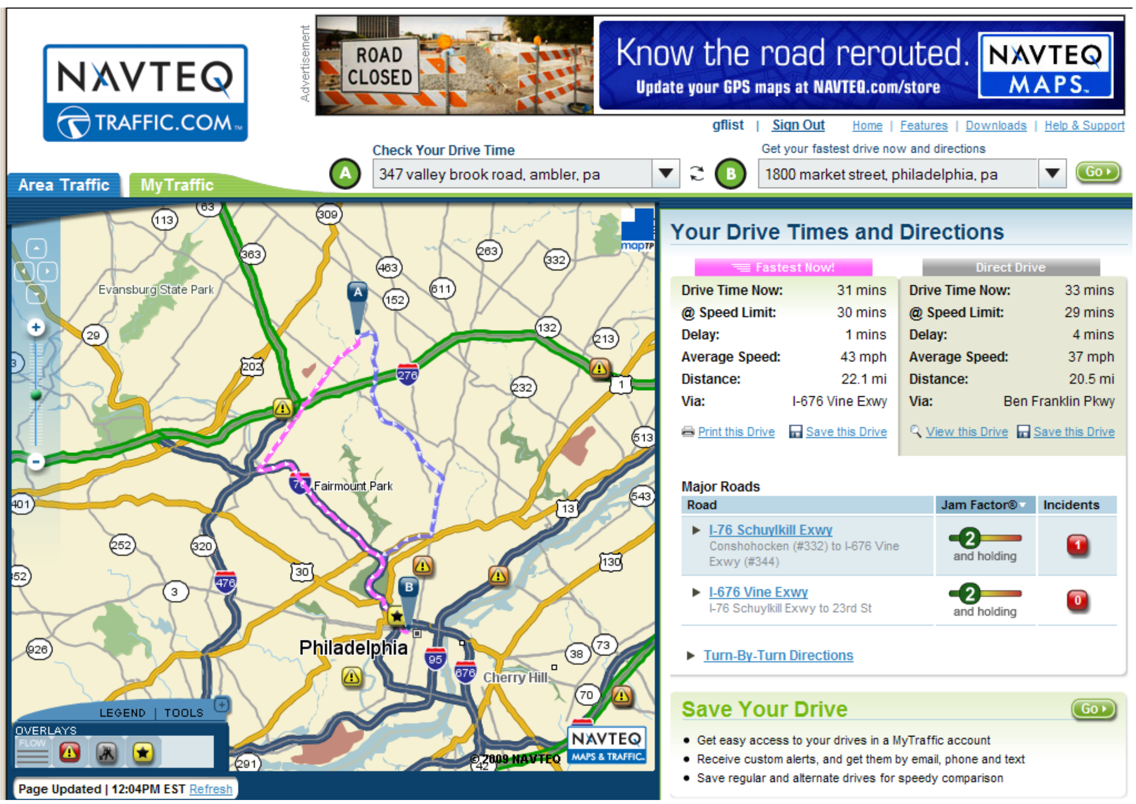

Source: www.traffic.com; accessed 6/22/2009.

Figure 34. An example of conveying travel time trends.

A display of speed trends is shown in Figure 35. The average from the current day (shown in red) is compared with the trailing 3-month average based on the day of the week (shown in green). In the case of the specific link queried, there was a significant drop in speed early in the morning that was strikingly different from the 3-month average.

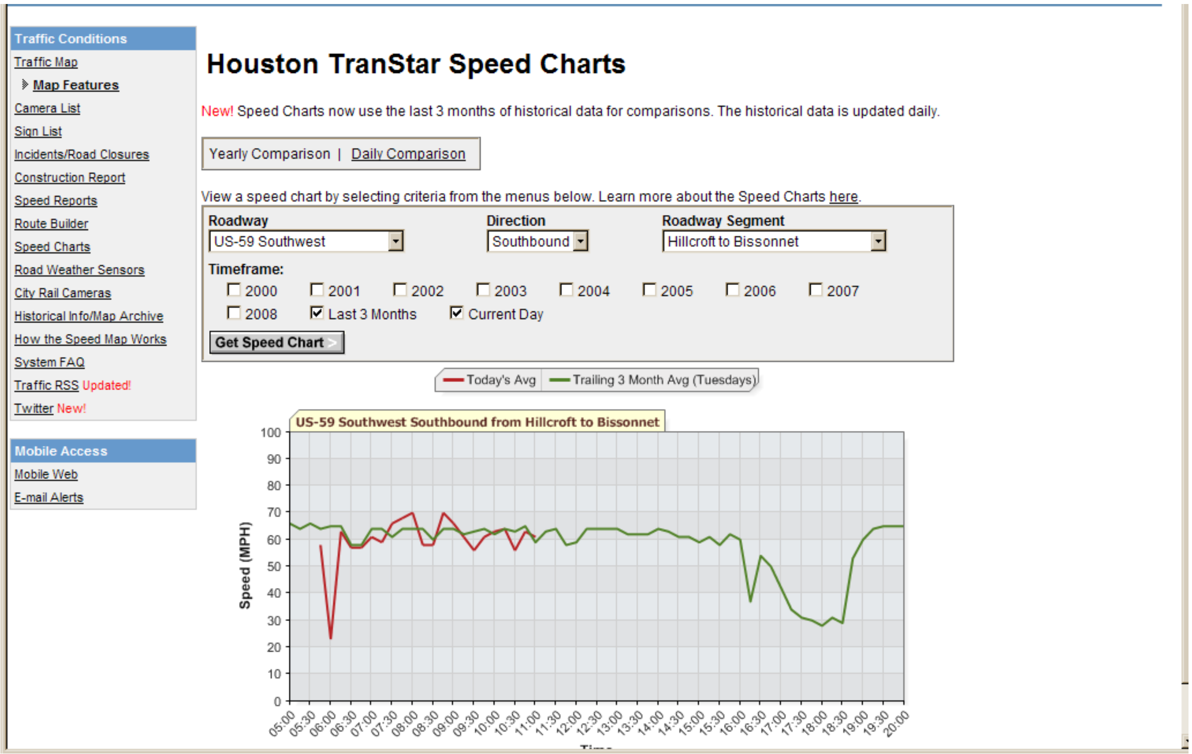

Source: http://traffic.houstontranstar.org/speedcharts/; accessed 6/22/2009.

Figure 35. A speed chart for a link in the Houston network.

A final display that is often used to portray variations in facility performance across distance and time is a speed contour plot. An illustration of this is shown in Figure 36. Distance (location) is on the horizontal axis, time is on the vertical axis. Darker colors indicate lower speeds and higher congestion. These low speeds are also likely to be an indicator of low reliability. The lighter colors imply higher speeds, correspondingly lower congestion, and most likely, better reliability.

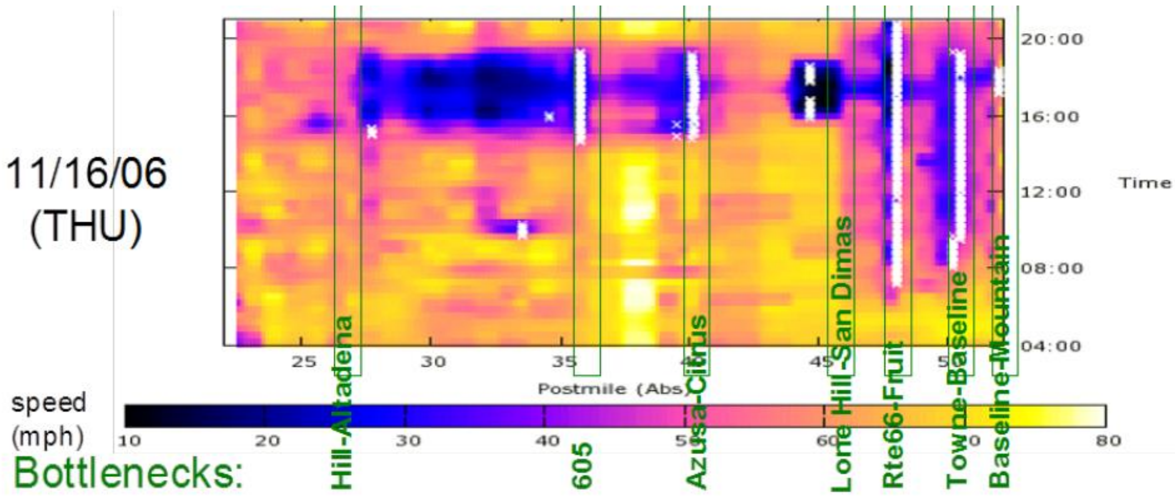

Source: Caltrans, I-210 CSMP.

Figure 36. A speed contour plot.

Summary and Conclusions

This handbook has illustrated ways in which travel time reliability information can be portrayed. Various audiences want to receive reliability information in different ways. Travelers and shippers want to know when they need to leave, or when the truck has to depart, in order to make an on-time arrival. Both groups also want to know what paths they should use to minimize the likelihood of encountering unforeseeable delays. Managing agencies want to know where the problem spots lie; where the network segments are that make the travel times vary.

The handbook endeavors to meet the needs of all these audiences ranging from novices to experts, from those for whom reliability is of cursory interest to those who want to understand all of the details and nuances. This means some of the presentation ideas are very simple, while others are more complex. Each is intended to be clear about what reliability information is being presented and how it should be interpreted.

The handbook is intended to be used both as a supplement to the materials developed in SHRP 2 L02 and as a stand-alone document. In light of the stand-alone objective, some redundancy exists with the L02 materials. Readers familiar with those materials can skip over the redundant discussions; but for readers for whom this as a stand-alone document, all of the material will be useful.

The displays that are presented have value because they can help agencies understand the reliability performance of their systems and monitor how reliability improves over time. It equips them to answer questions like the following:

- What is the distribution of travel times in the system?
- How is the distribution of travel times (or rates) affected by recurrent congestion and nonrecurring events?

- How are freeways and arterials performing relative to reliability performance targets set by the agency?
- Are capacity investments and other operational actions helping to improve the reliability of the travel times?
- Are operational improvement actions and capacity investments helping to improve the travel times and their reliability?

Related References

Bates, J., Polak, J., Jones, P. and Cook, A. 2001. The valuation of reliability for personal travel, *Transportation Research, Part E*, Vol. 37, pp. 191–229.

Batley, R., and Ibanez, J. N. 2009. Randomness in preferences, outcomes and tastes; an application to journey time risk. *Proceedings of the International Choice Modelling Conference*, Harrogate, UK.

Berkow, M., Wolfe, M., Monsere, C., and Bertini, R. 2008. Using signal system data and buses as probe vehicles to define the congested regime on arterials. *Proceedings of the 87th Annual Meeting of the Transportation Research Board*, Washington, D.C.

Bertini, R. L., and Ahmed El-Geneidy, M. 2003. Generating Transit Performance Measures with Archived Data.

Bertini, R. L., and Ahmed El-Geneidy, M. 2004. Modeling Transit Trip Time Using Archived Bus Dispatch System Data.

Bertini, R. L., Cameron, G. J., and Peters, J. 2005. Evaluating traffic signal improvements using archived transit AVL data. *ITE Journal,* Vol.75, No. 2, pp. 69–75.

Bo, L., and Hiroaki, M. 2008. Discussion of traffic signal effect on calculating link travel time and field test evaluation. *Proceedings 8th International Conference on Intelligent Transport System Telecommunications,* pp. 112–115.

Briggs, V., and Walton, C. M. 2000. The Implications of Privacy Issues for Intelligent Transportation Systems (ITS) Data. Research Report 472840-00075, Center for Transportation Research.

Byon, Y.-J., Shalaby, A., and Abdulhai, B. 2006. Travel Time Collection and Traffic Monitoring via GPS Technologies. *Proceedings of the IEEE Intelligent Transportation Systems Conference.*

Cambridge Systematics, Texas A&M Transportation Institute, University of Washington, and Dowling Associates. 2003. *Providing a Highway System with Reliable Travel Times Prepared for the Future*. Strategic Highway Research Program NCHRP Project 20-58, Transportation Research Board, Washington, D.C.

Cambridge Systematics and Texas A&M Transportation Institute. 2005. *Traffic Congestion and Reliability: Trends and Advanced Strategies for Congestion Mitigation*. Prepared for the FHWA Office of Operations, Washington, D.C.

Cambridge Systematics, Texas A&M Transportation Institute, University of Washington, Dowling Associates, Street Smarts, Levinson, H., and Rakha, H. 2013. *SHRP 2 Report S2-L03*-RR: *Analytical Procedures for Determining the Impacts of Reliability Mitigation Strategies*. Transportation Research Board of the National Academies, Washington, D.C.

Carrion, C., and Levinson, D. 2010. Value of reliability: High occupancy toll lanes, general purpose lanes, and arterials. *Proceedings of 4th International Symposium Transportation Network Reliability*, Minneapolis, Minn.

Carrion, C., and Levinson, D. 2011. A model of bridge choice across the Mississippi River in Minneapolis, Presented at the 90th Annual Transportation Research Board Conference, Washington, D.C.

Cetin, M., List, G. F., and Zhou, Y. 2005. Factors affecting minimum number of probes required for reliable estimation of travel time. *Transportation Research Record,* Vol. 1917, pp. 37–44.

Chakroborty, P., and Kikuchi, S. 2004. Using bus travel time data to estimate travel times on urban corridors. *Transportation Research Record,* Vol.1870, pp. 8–25.

Chang, X., and Stopher, P. 1981. Defining the perceived attributes of travel modes for urban work trips, *Transportation Planning and Technology*, Vol. 7, pp. 55–65.

Chen, C., Kwon, J., Skabardonis, A., and Varaiya, P. 2003. Detecting Errors and Imputing Missing Data for Single Loop Surveillance Systems. *Transportation Research Record,* Vol. 1855, pp. 160–167.

De Fabritiis, C., Ragona, R., and Valenti, G. 2008. Traffic estimation and prediction based on real time floating car data. *Proceedings of IEEE Conference on Intelligent Transportation Systems*, pp. 197–203.

Demers, A., List, G. F., Wallace, W. A., Lee, E. E., and Wojtowicz, J. 2006. Probes as path seekers: a new paradigm. *Transportation Research Record,* Vol. 1944, pp. 107–114.

Demers A., List, G. F., Wojtowicz, W., Kornhauser, A., Wallace, W. A., Lee, E. E., and Salasznyk, P. 2006. Experimenting with real-time ATIS: Stepping forward from ADVANCE. *Proceedings of the 9th International Conference on Applications of Advanced Technology in Transportation*.

Dhaene, J., Denuit, M., Goovaerts, M. J., Kaas, R., and Vyncke, D. 2002a. The concept of comonotonicity in actuarial science and finance: theory. *Insurance: Mathematics and Economics*, Vol. 31, No.1, pp. 3–33.

Dhaene, J., Denuit, M., Goovaerts, M. J., Kaas, R, and Vyncke, D. 2002b. The concept of comonotonicity in actuarial science and finance: applications, *Insurance: Mathematics and Economics*, Vol. 31, No. 2, pp. 133–161.

Dion F., and Rakha, H. 2006. Estimating dynamic roadway travel times using automatic vehicle identification data for low sampling rates. *Transportation Research Part B*, Vol. 40, No.9, pp. 745–766.

Dong, J., Mahmassani, H. S. 2011. Stochastic modeling of traffic flow breakdown phenomenon: Application to predicting travel time reliability. *Proceedings of 14th International IEEE Conference on Intelligent Transportation Systems*, pp. 2112–2117.

Ebeling, C. E. 1997. *An Introduction to Reliability and Maintainability Engineering*. McGraw Hill.

Enam, E., and Al-Deek, H. 2006. Using Real-Life Dual-Loop Detector Data to Develop New Methodology for Estimating Freeway Travel Time Reliability. *Transportation Research Record 1959*, pp. 140–150.

Ernst, J. M., Day, C. M., and Krogmeier, J. V. 2012. Probe Data Sampling Guidelines for Characterizing Arterial Travel Time. *Proceedings of the 91st Annual Meeting of the*

Transportation Research Board, Washington, D.C.

Federal Highway Administration. 2005. Traffic Congestion and Reliability: Trends and Advanced Strategies for Congestion Mitigation. September 2005.

Federal Highway Administration. 2008. Travel time reliability: Making it there on time, all the time. Available online at ops.fhwa.dot.gov/publications/tt_reliability/TTR_Report.htm#WhatisTTR.

Feng, Y., Davis, G.A., and Hourdos, J. 2011. Arterial Travel Time Characterization and Real Time Traffic Condition Identification Using GPS-equipped Probe Vehicles. *Proceedings of the 90th Annual Transportation Research Board Meeting*, Washington, D.C.

Feng, Y., Hourdos, J., and Davis, G. A. 2012. A Bayesian Model for Constructing Arterial Travel Time Distributions using GPS Probe Vehicles. *Proceedings of the 91st Annual Meeting of the Transportation Research Board*, Washington, D.C.

Fontaine, M. D., and Smith, B. L. 2005. Probe-based traffic monitoring systems with wireless location technology. *Transportation Research Record,* Vol. 1925, pp. 3–11.

Fosgerau, M., and Karlstrom, A. 2010. The value of reliability. *Transportation Research Part B*, Vol. 44, pp. 38–49.

Fosgerau, M., and Engelson, L. 2011. The value of travel time variance. *Transportation Research Part B*, Vol. 45, pp. 1–8.

Fraley, C., and Raftery A. E. 2009. MCLUST Version 3 for R: Normal Mixture Modeling and Model-Based Clustering. Technical Report No. 504. Department of Statistics, University of Washington. http://www.stat.washington.edu/fraley/mclust/tr504.pdf.

Gaver, D. 1968. Headstart strategies for combating congestion. *Transportation Science*, Vol. 2, pp. 172–181.

Guo, F., Rakha, H., and Park, S. 2010. A Multi-State Travel Time Reliability Model. *Transportation Research Record,* Vol. 2188, pp. 46-54.

Guo, F., Li, Q., and Rakha, H. 2012. Multi-state Travel Time Reliability Models with Skewed Component Distributions. *Proceedings of the 91st Annual Meeting of the Transportation Research Board*, Washington, D.C.

Haas, R., Carter, M., Perry, E., Trombly, J., Bedsole, E., and Margiotta, R. iFlorida. 2009. Model Deployment Evaluation Report. Prepared for the USDOT. Report No FHWA-HOP-08-050. January.

Haghani, A., Hamedi, M., Sadabadi, K. F., Young, S., and Tarnoff, P. 2010. Data Collection of Freeway Travel Time Ground Truth with Bluetooth Sensors. In *Transportation Research Record: Journal of the Transportation Research Board, No. 2160*, Transportation Research Board of the National Academies, Washington, D.C., pp. 60–68.

Hainen, A. M., Remias, S. M., Brennan, T. M., Day, C. M., and Bullock, D. M. 2012. Probe vehicle data for characterizing road conditions associated with inclement weather to improve road maintenance decisions. *Proceedings of IEEE Intelligent Vehicles Symposium*, pp. 730–735.

Hall, R., and Nilesh, V. 2000. Buses as a traffic probe demonstration project. *Transportation Research Record,* Vol. 1731, pp. 96–103.

Haseman, R. J., Wasson, J. S., and Bullock, D. M. 2010. Real-time measurement of travel time delay in work zones and evaluation metrics using Bluetooth probe tracking. *Transportation Research Record*, Vol. 2169, pp. 40–53.

Hellinga, B. R., and Fu, L. 2002. Reducing bias in probe-based arterial link travel time estimates. *Transportation Research Part C,* Vol. 10, No. 4, pp. 257–273.

Hesham, R., Ihab, E-S., Mazen, A., and Dion, F. 2006. Estimating Path Travel Time Reliability. *Intelligent Transportation Systems Conference Proceedings*, pp. 236–241.

Higatani, A., Kitazawa, T., Tanabe, J., Suga, Y., Sekhar, R., and Asakura, Y. 2009. Empirical analysis of travel time reliability measures in Hanshin expressway network. *Journal of Intelligent Transportation Systems: Technology, Planning, and Operations*, Vol. 13, No. 1, pp. 28–38.

Hoeitner, A., Herringy, R., Bayenz, A., Hanx, Y., Moutardex, F., and de La Fortellex, A. 2012. Large scale estimation of arterial traffic and structural analysis of traffic patterns using probe vehicles. *Proceedings of the 91st Annual Meeting of the Transportation Research Board*, Washington, D.C.

Ishak, S., Kondagari, S., and Alecsandru, C. 2007. Probabilistic data-driven approach for real-time screening of freeway traffic data. *Transportation Research Record*, Vol. 2012, pp. 94–104.

Jackson, W., and Jucker, J. 1982. An empirical study of travel time variability and travel choice behavior, *Transportation Science*, Vol. 16, pp. 460–475.

Jenelius, E., Mattsson, L. G., and Levinson, D. 2011. Traveler delay costs and value of time with trip chains, flexible activity scheduling and information. *Transportation Research Part B*, Vol. 45, pp. 789–807.

Jintanakul, K., Chu, L., and Jayakrishnan, R. 2009. Bayesian Mixture Model for Estimating Freeway Travel Time Distributions from Small Probe Samples from Multiple Days. *Transportation Research Record,* Vol. 2136, pp. 37–44.

Kaparias, I., Bell, M. G. H., and Belzner, H. 2008. A new measure of travel time reliability for in-vehicle navigation systems. *Journal of Intelligent Transportation Systems: Technology, Planning, and Operations*, Vol. 12, No. 4, pp. 202–211.

Karr, A. F. 1993. *Probability.* Springer–Verlag, New York.

Karr, A. F., Sanil, A. P., and Banks, D. L. 2006. Data quality: A statistical perspective. *Statistical Methodology*, Vol. 3, No. 2, pp. 137–173.

Karr, A. F., Fulp, W. J., Lin, X., Reiter, J. P., Vera, F., and Young, S. S. 2007. Secure, privacy-preserving analysis of distributed databases. *Technometrics*, Vol.49, No. 3, pp. 335–345.

Khattak, A., Youngbin, Y., and Linda, S. 2003. Willingness to pay for travel information. *Transportation Research Part C*, Vol. 11, No. 2, Pergamon Press, pp. 137–159.

Khattak, A. J., Fan, Y., and Teague, C. (2008). Economic impact of traffic incidents on businesses. *Transportation Research Record, 2067*, pp. 93–100.

Khattak, A. J., Joseph, L. S., and Koppelman, F. S. 1994. Effect of Traffic Information on Commuters' Propensity to Change Route and Departure Time. *Journal of Advanced Transportation*, Vol. 29, No. 2, pp. 193–212.

Kwon, J., Coifman, B., and Bickel, P. 2000. Day-to-day travel-time trends and travel-time prediction from loop-detector data. *Transportation Research Record 1717,* pp. 120–129.

Kwon, J., Petty, K., and Varaiya, P. 2007. Probe Vehicle Runs or Loop Detectors? Effect of Detector Spacing and Sample Size on Accuracy of Freeway Congestion Monitoring, *Transportation Research Record 2012*, pp. 57–63.

Leng, J., Zhang, Y., and Leng, Y. 2009. Assessment methodology for road network travel time reliability under ice and snowfall conditions. *Proceedings of the 9th International Conference of Chinese Transportation Professionals*, Vol. 358, pp. 1124–1130.

Li, R., Rose, G., and Sarvi, M. 2006. Using automatic vehicle identification data to gain insight into travel time variability and its causes. *Transportation Research Record 1945*, pp. 24–32.

Lin, W., Kulkarni, A., and Mirchandani, P. 2003. Arterial travel time estimation for advanced traveler information systems. *Proceedings of the 82nd Annual Meeting of the Transportation Research Board*. Washington, D.C.

List, G. F., Wallace, W. A., Demers, A., Salasznyk, P., Lee, E. E., and Wojtowicz, J. 2005. Field experiment with a wireless GPS-based ATIS system. *Proceedings of the 12th World Congress on ITS*, San Francisco, Calif.

List, G. F., Demers, A., Wallace, W. A., Lee, E. E., and Wojtowicz, J. 2005. ATIS via wireless probes: smart vehicles for smart travelers. *INFORMS Annual Meeting*.

List, G. F., and Demers, A. 2006. Estimating highway facility performance from AVL data. *Proceedings of the Fifth International Symposium on Highway Capacity and Quality of Service*, pp. 319–328, Osaka, Japan.

List, G. F., B. Williams, N. Rouphail, R. Hranac, T. Barkley, E. Mai, A. Ciccarelli, L. Rodegerdts, K. Pincus, B. Nevers, A. F. Karr, X. Zhou, J. Wojtowicz, J. Schofer, and A. Khattak. *SHRP 2 Report S2-L02-RR-1: Establishing Monitoring Programs for Travel Time Reliability.* Transportation Research Board of the National Academies, Washington, D.C., 2014.

List, G. F., B. Williams, N. Rouphail, R. Hranac, T. Barkley, E. Mai, A. Ciccarelli, L. Rodegerdts, K. Pincus, B. Nevers, A. F. Karr, X. Zhou, J. Wojtowicz, J. Schofer, and A. Khattak. *SHRP 2 Report S2-L02-RR-2: Guide for Establishing Monitoring Programs for Travel Time Reliability.* Transportation Research Board of the National Academies, Washington, D.C., 2014.

Liu, K., Yamamoto, T., and Morikawa, T. 2007. Feasibilities and challenges of probe technologies for real-time traffic data collection. *Proceedings of the 7th International Conference of Chinese Transportation Professionals Congress*, pp. 328–340.

Liu, H., Sang, L., Zhang, K., and Yuan, Y. 2010. An evaluation of obtaining travel time observations via new technology: a case study in Tianjin. *Proceedings of the 10th International Conference of Chinese Transportation Professionals*, Vol. 382, pp. 2380–2388.

Lomax, T., Schrank, D., Turner, S., and Margiotta, R. 2003. *Selecting Travel Reliability Measures*. http://ttitamuedu/documents/474360-1pdf.

Lyman, K., and Bertini, R. L. 2008. Using travel time reliability measures to improve regional transportation planning and operations. *Transportation Research Record 2046*, pp. 1–10.

Ma, X., and Koutsopoulos, H. N. 2010. Estimation of the automatic vehicle identification based spatial travel time information collected in Stockholm. *IET Intelligent Transport Systems*, Vol. 4, No. 4, pp. 298–306.

Ma, Y., Chowdhury, M., Sadek, A., and Jeihani, M. 2009. Real-time highway traffic condition assessment framework using vehicle infrastructure integration (VII) with artificial intelligence (AI). *IEEE Transactions on Intelligent Transportation Systems*, Vol. 10, No. 4, pp. 615–627.

Margiotta, R., Lomax, T., Hallenbeck, M., Turner, S., Skabardonis, A., Ferrell, C., and Eisele, B. 2006. *Guide to Effective Freeway Performance Measurement*, Final Report, NCHRP Project 3–68, Transportation Research Board, Washington, D.C.

Martchouk, M., Mannering, F., and Bullock, D. 2011. Analysis of Freeway Travel Time Variability Using Bluetooth Detection. *Journal of Transportation Engineering*, Vol. 137, No. 10, pp. 697–704.

Morris, A. G., Kornhauser, A. L., and Kay, M. J. 1998. Urban freight mobility: collection of data on time, costs, and barriers related to moving product into the central business district. *Transportation Research Record,* Vol. 1613, pp. 27–32.

National Institute of Statistical Sciences. 2004. Data Confidentiality, Data Quality and Data Integration for Federal Databases: Foundations to Software Prototypes. Available online at www.niss.org/dgii.

Noland, R., and Small, K. 1995. Travel-time uncertainty, departure time choice, and the cost of morning commutes. *Transportation Research Record*, Vol. 1493, pp. 150–158.

Pan, C., Lu, J., Wang, D., and Ran, B. 2007. Data collection based on global positioning system for travel time and delay for arterial roadway network. *Transportation Research Record 2024*, pp. 35–43.

Park, M., Kim, S., Park, C., and Chon, K. 2007. Transportation network design considering travel time reliability. *Proceedings of the 10th International IEEE Conference on Intelligent Transportation Systems*, pp. 496–502.

Prashker, J. 1979. Direct analysis of the perceived importance of attributes of reliability of travel modes in urban travel. *Transportation*, Vol. 8, pp. 329–346.

Pu, W. 2011. Analytic Relationships between Travel Time Reliability Measures. *Transportation Research Record 2254*, pp. 122–130.

Quiroga, C. A., and Bullock, D. 1998. Travel time studies with global positioning and geographic information systems: an integrated methodology. *Transportation Research Part C*, Vol. 6, No.1/2, 101–127.

Ramezani, M., and Geroliminis, N. 2012. Estimation of arterial route travel time distribution with Markov chains. *Proceedings of the 91st Annual Meeting of the Transportation Research Board*, Washington, D.C.

Rice, J., and Van Zwet, E. 2004. A simple and effective method for predicting travel times on freeways. *IEEE Transactions on Intelligent Transportation Systems*, Vol. 5, No. 3, pp. 200–207.

Rosenblatt, M. 1956. Remarks on some nonparametric estimates of a density function. *Annals of Mathematical Statistics,* Vol. 27, pp. 832–837.

Shen, L., and Hadi, M. 2012. Practical approach for travel time estimation from point traffic detector data. *Journal of Advanced Transportation*.

Silverman, B. W. 1986. *Density Estimation for Statistics and Data Analysis*, Chapman & Hall, London.

Small, K. 1982. The scheduling of consumer activities: Work trips. *American Economic Review*, Vol. 72, pp. 467–479.

Small, K., Winston, C., and Yan, J. 2005. Uncovering the distribution of motorists' preferences for travel time and reliability. *Econometrica*, Vol. 73, pp. 1367–1382.

Small, K., and Verhoef, E. 2007. *The Economics of Urban Transportation.*, Routledge, Taylor & Francis Group, New York.

Soriguera, F., and Thorson, L. 2007. Travel time measurement using toll infrastructure. *Transportation Research Record 2027*, pp. 99–107.

Soriguera, F. 2011. Highway travel time accurate measurement and short-term prediction using multiple data sources. *Transportmetrica*, Vol. 7, No. 1, pp. 85–109.

Sun, H., and Gao, Z. 2012. Stochastic traffic equilibrium based on travel time robust reliability. *Journal of Transportation Systems Engineering and Information Technology*, Vol. 12, No. 2, pp. 76–84.

Susilawati, S., Taylor, M. A. P., and Somenahalli, S. V. C. 2011. Distributions of travel time variability on urban roads. *Journal of Advanced Transportation*, doi: 101002/atr192.

Tilahun, N., and Levinson, D. 2010. A moment of time: Reliability in route choice using stated preference. *Journal of Intelligent Transportation Systems*, Vol. 14, pp. 179 –187.

Transportation Research Center. 2009. *Improving Reliability on Surface Transportation Networks: Summary Document*, OECD.

Transportation Research Center. 2010. *Improving Reliability on Surface Transportation Networks*, OECD.

Tseng, Y., and Verhoef, E. 2008. Value of time by time of day: a stated-preference study. *Transportation Research Part B*, Vol. 42, pp. 607–618.

Tsubota, T., Kikuchi, H., Uchiumi, K., Warita, H., and Kurauchi, F. 2011. Benefit of Accident Reduction Considering the Improvement of Travel Time Reliability. *International Journal of Intelligent Transportation Systems Research*, Vol. 9, No. 2, pp. 64–70.

Tu, H., Van Lint, H., and van Zuylen, H. 2008. The effects of traffic accidents on travel time reliability. *Proceedings of IEEE Conference on Intelligent Transportation Systems*, pp. 79–84.

Uno, N., Kurauchi, F., Tamura, H., and Iida, Y. 2009. Using bus probe data for analysis of travel time variability. *Journal of Intelligent Transportation Systems: Technology, Planning, and Operations*, Vol. 13, No. 1, pp. 2–15.

Vanajakshi, L., Subramanian, S. C., and Sivanandan, R. 2009. Travel time prediction under heterogeneous traffic conditions using global positioning system data from buses. *IET Intelligent Transport Systems,* Vol. 3, No. 1, pp. 1–9.

Van Hinsbergen, C. P. I. J., and Van Lint, J. W. C. 2008. Bayesian combination of travel time prediction models. *Transportation Research Record*, Vol. 2064, pp. 73–80.

Van Lint, J. W. C., and van Zuylen, H. J. 2005. Monitoring and Predicting Freeway Travel Time Reliability Using Width and Skew of Day-to-Day Travel Time Distribution. *Transportation Research Record 1917*, pp. 54–62.

Van Lint, J. W. C., van Zuylen, H. J., and Tu, H. 2008. Travel time unreliability on freeways: Why measures based on variance tell only half the story. *Transportation Research Part A,* Vol. 42, No. 1, pp. 258–277.

Van Zwet, E., Chen, C., Jia, Z., and Kwon, J. 2003. A statistical method for estimating speed from single loop detectors. Freeway Performance Measurement System (PeMS). http://pems.eecs.berkeley.edu.

Vaziri, M., and Lam., T. N. 1983. Perceived factors affecting driver route decisions. *Journal of Transportation Engineering*, Vol. 109, p. 297–311.

Vickrey, W. 1969. Congestion theory and transport investment. *American Economic Review*, Vol. 59, pp. 251–260.

Wang, J., Zou, N., and Chang, G. 2008. Travel time prediction: Empirical analysis of missing data issues for advanced traveler information system applications. *Transportation Research Record*, Vol. 2049, pp. 81–91.

Wang, J., Sun, G., and Hu, X. 2009. Analysis of city transportation networks' travel time reliability during adverse weather. *Proceedings of the 9th International Conference of Chinese Transportation Professionals*, Vol. 358, pp. 1536–1542.

Wang, J., He, J., and Wu, L. 2011. Evaluating approach of travel time reliability for highway network under rain environment. *Journal of Transportation Systems Engineering and Information Technology,* Vol. 11, No. 6, pp. 117–123.

Wasson, J. S., Sturdevant, J. R., and Bullock, D. M. 2008. Real-time travel time estimates using media access control address matching. *ITE Journal*, Vol. 78, No. 6, pp. 20–23.

Wikipedia, "Harvey Balls," http://en.wikipedia.org/wiki/Harvey_Balls, accessed 2014.

Wojtowicz, J., Murrugarra, R. I., Bertoli, B., Wallace, W. A., Manuel, P., He, W., and Body, C. 2008. RFID technology for AVI: field demonstration of a wireless solar powered E-ZPass tag reader. *Proceedings of the 15th World Congress on Intelligent Transport Systems*.

Wosyka, J., and Pribyl, P. 2012. Real-time travel time estimation on highways using loop detector data and license plate recognition. *Proceedings of 9th International Conference*, ELEKTRO, pp. 391–394.

Xiaoliang, M., and Koutsopoulos, H. N. 2008. A new online travel time estimation approach using distorted automatic vehicle identification data. *Proceedings of IEEE Conference on Intelligent Transportation Systems,* pp. 204–209.

Xiong, Z., Shao, C., and Yao, Z. 2007. The framework of assessment on travel time reliability. *Proceedings of International Conference on Transportation Engineering,* pp. 223–228.

Yamamoto, T., Liu, K., and Morikawa, T. 2006. Variability of travel time estimates using probe vehicle data. *Proceedings of the Fourth International Conference on Traffic and Transportation Studies*, pp. 278–287.

Yamazaki, H., Uno, N., and Kurauchi, F. 2012. The effect of a new intercity expressway based on travel time reliability using electronic toll collection data. *IET Intelligent Transportation Systems*, Vol. 6, No. 3, pp. 306–317.

Yan, Y., Guo, X., Li, Y., Kong, Z., and He, M. 2012. Bus transit travel time reliability evaluation based on automatic vehicle location data. *Journal of Southeast University*, Vol. 28, No. 1, pp. 100–105.

Yang, M., Liu, Y., and You, Z. 2010. The reliability of travel time forecasting. *IEEE Transactions on Intelligent Transportation Systems,* Vol. 11, No. 1, pp. 162–171.

Yang, Y., Yao, E., Qu, D., and Zhang, Y. 2011. Study on travel time reliability of probe vehicle system based on minimum sample size analysis. Multimodal Approach to Sustained Transportation System Development—Information, Technology, Implementation—*Proceedings of the First International. Conference on Transportation Information and Safety*, pp. 1680–1686.

Zegeer, J., J. Bonneson, R. Dowling, P. Ryus, M. Vandehey, W. Kittelson, N. Rouphail, B. Schroeder, A. Hajbabaie, B. Aghdashi, T. Chase, S. Sajjadi, R. Margiotta, and L. Elefteriadou. 2014. *SHRP 2 Report S2-L08-RW-1: Incorporating Travel Time Reliability into the* Highway Capactiy Manual. Transportation Research Board of the National Academies, Washington, D.C.

Zou, N., Wang, J., and Chang, G. 2008. A reliable hybrid prediction model for real-time travel time prediction with widely spaced detectors. *Proceedings of IEEE Conference on Intelligent Transportation Systems,* pp. 91–96.

Zou, N., Wang, J., Chang, G., and Paracha, J. 2009. Application of advanced traffic information systems: Field test of a travel-time prediction system with widely spaced detectors. *Transportation Research Record 2129*, pp. 62–72.